Supporting Information

Planar Chiral Ferrocenylphosphine-borane Complexes Featuring Agostic-type B–H···E (E = Hg, Sn) Interactions

Alain C. Tagne Kuate,[a,b] Roger A. Lalancette,[a]* F. Jäkle[a]*

[a]Department of Chemistry, Rutgers University-Newark, 73 Warren Street, Newark, NJ 07102, USA

[b]Department of Chemistry, Faculty of Sciences, University of Dschang, P.O. Box 67, Dschang, Cameroon

* To whom correspondence should be addressed.
Email: fjaekle@andromeda.rutgers.edu ; rogerlal@andromeda.rutgers.edu

Reaction of *rac*-5 with $PhBCl_2$: Isolation of $FcPPh_2{\cdot}BH_3$

During the course of our studies we also attempted the synthesis of boron-bridged diferrocenes. However, we could only isolate the parent species $FcPPh_2{\cdot}BH_3$, presumable due to protonolysis. The lack of analytical data on $FcPPh_2{\cdot}BH_3$ in the literature encouraged us to perform a full characterization. The MALDI-TOF mass spectrum of $FcPPh_2{\cdot}BH_3$ showed a molecular ion peak at m/z = 767.5008, suggesting the presence of a dimer with loss of H_2.

Synthetic Procedure: A solution of *rac*-**5** (0.052 g, 0.084 mmol) in toluene (10 mL) was slowly added to a solution of $PhBCl_2$ (0.007 g, 0.042 mmol, 0.5 equiv) in toluene (2 mL) at –27 ^oC inside a glovebox. The mixture was stirred at room temperature for two days and heated at 90 ^oC overnight in a sealed flask. A grey solid was formed, which was removed by filtration and the solvent was evaporated in vacuum to leave a yellow-orange residue. The latter was taken in a minimum of THF and passed through a plug of Al_2O_3 eluted with THF/hexane. The first band was concentrated, dissolved in CH_2Cl_2, layered with hexanes and stored at –25 ^oC. An orange solid crystallized that was identified to be ferrocenylphosphine-borane adduct $FcPPh_2{\cdot}BH_3$. Yield: 0.023 g (69%). ^1H NMR (499.9 MHz, $CDCl_3$, 25 ^oC): δ = 7.59 (m, 4H, Ph), 7.47 (m, 2H, Ph), 7.41 (m, 4H, Ph), 4.51 (nr, 2H, Cp), 4.42 (nr, 2H, Cp), 4.10 (s, 5H, free Cp), 1.25 (brm, 3H, BH_3). $^{13}C\{^1H\}$ NMR (125.7 MHz, $CDCl_3$, 25 ^oC): δ = 133.0 (d, $^2J_{P,C}$ = 9 Hz, *o*-Ph), 131.7 (d, $^1J_{P,C}$ = 59 Hz, *i*-Ph), 131.2 (s, *p*-Ph), 128.8 (d, $^3J_{P,C}$ = 10 Hz, *m*-Ph), 73.1 (d, $J_{P,C}$ = 10 Hz, Cp), 72.2 (d, $^1J_{P,C}$ = 8 Hz, Cp), 70.1 (s, free Cp), 69.1 (d, $^1J_{P,C}$ = 69 Hz, *i*-Cp-P). $^{31}P\{^1H\}$ NMR (202.5 MHz, $CDCl_3$, 25 ^oC): δ = 16.0 (nr). $^{11}B\{^1H\}$ NMR (160.4 MHz, $CDCl_3$, 25 ^oC): –38.4 (nr). High-resolution MALDI-TOF MS (positive mode, anthracene): m/z 370.0545 ($[(FcPPh_2)+H]^+$, 100%, calcd for $^{12}C_{22}{}^1H_{19}{}^{11}B^{56}Fe^{31}P$ 370.0568).

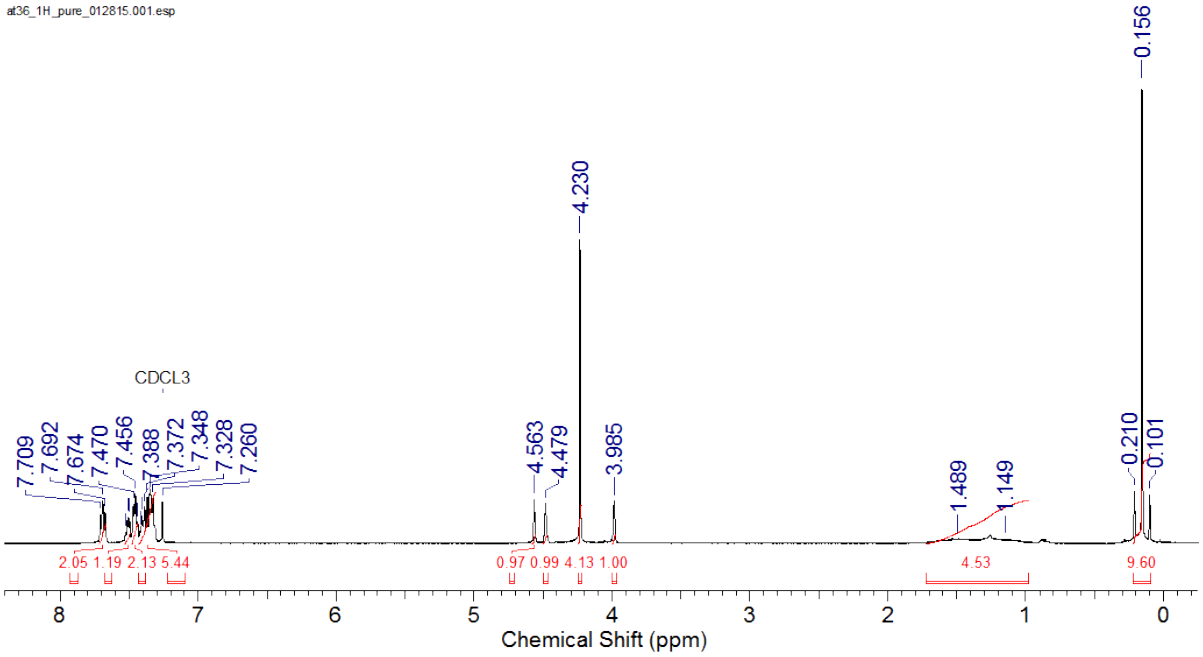

Figure S1. ^{1}H NMR spectrum of (p*S*)-**3**.

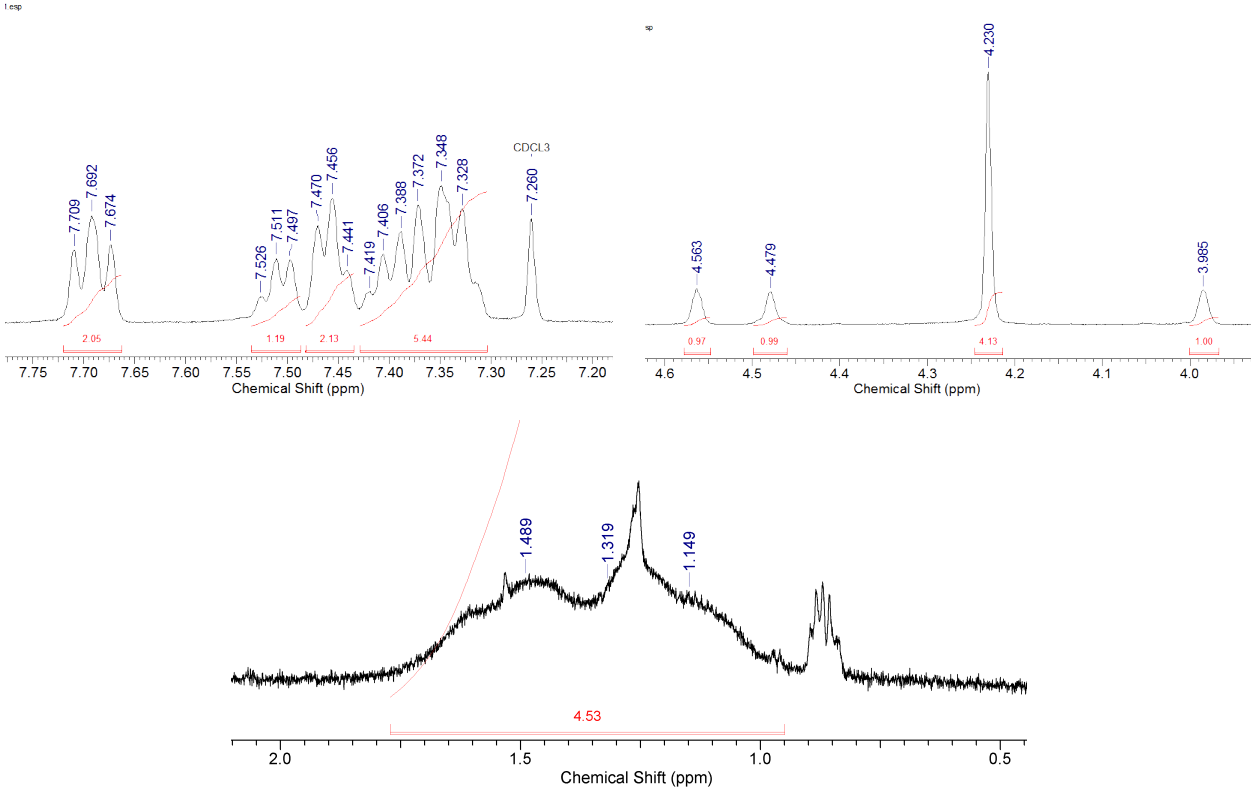

Figure S2. Expansions of the ^{1}H NMR spectrum of (p*S*)-**3**.

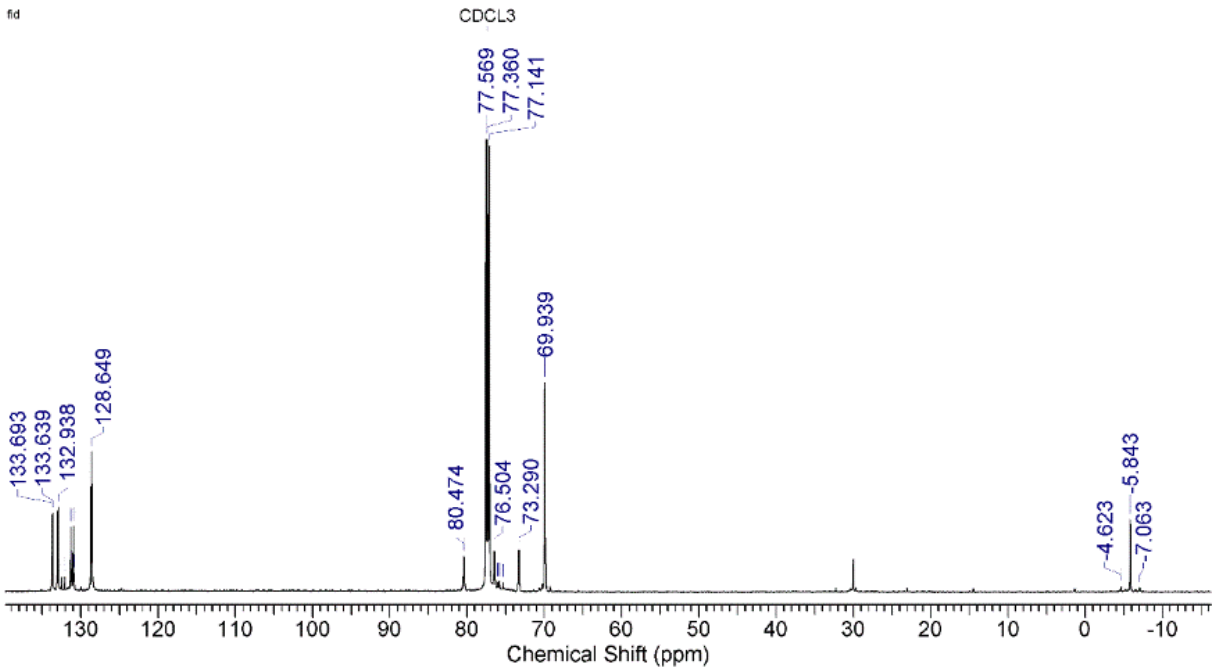

Figure S3a. ^{13}C NMR spectrum of (p*S*)-**3**.

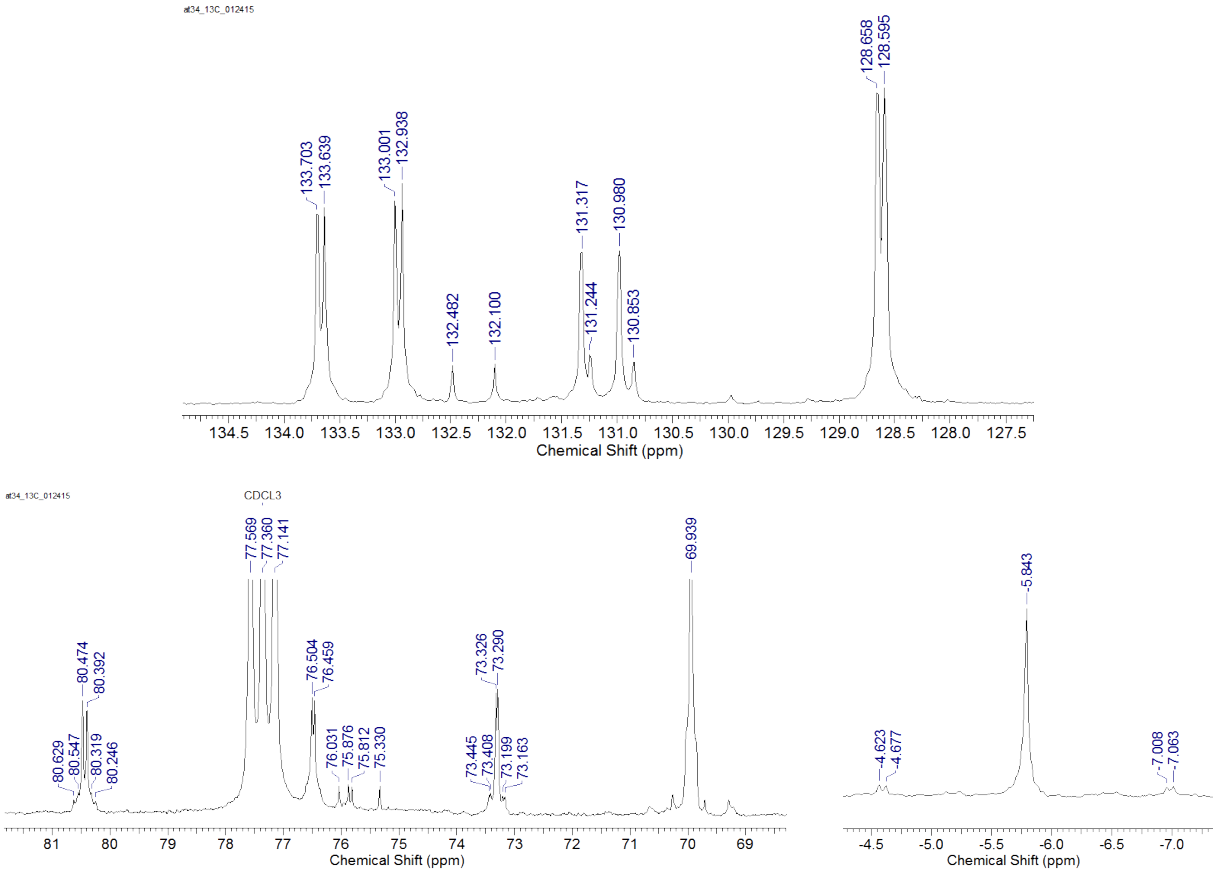

Figure S3b. Expansions of the ^{13}C NMR spectrum of (p*S*)-**3**.

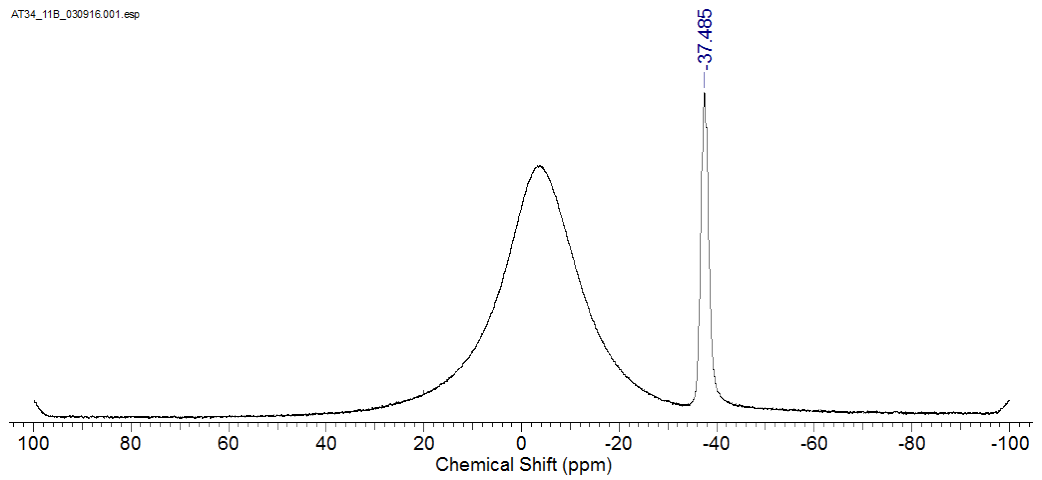

Figure S4. ^{11}B NMR spectrum of (p*S*)-**3**.

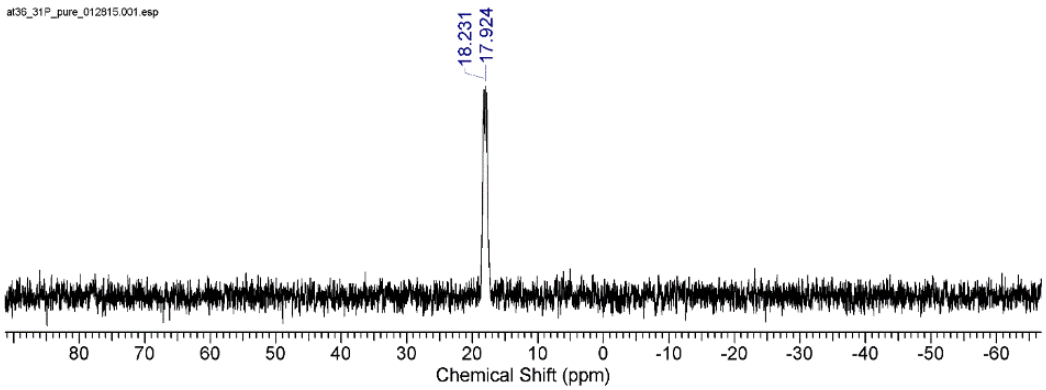

Figure S5. ^{31}P NMR spectrum of (p*S*)-**3**.

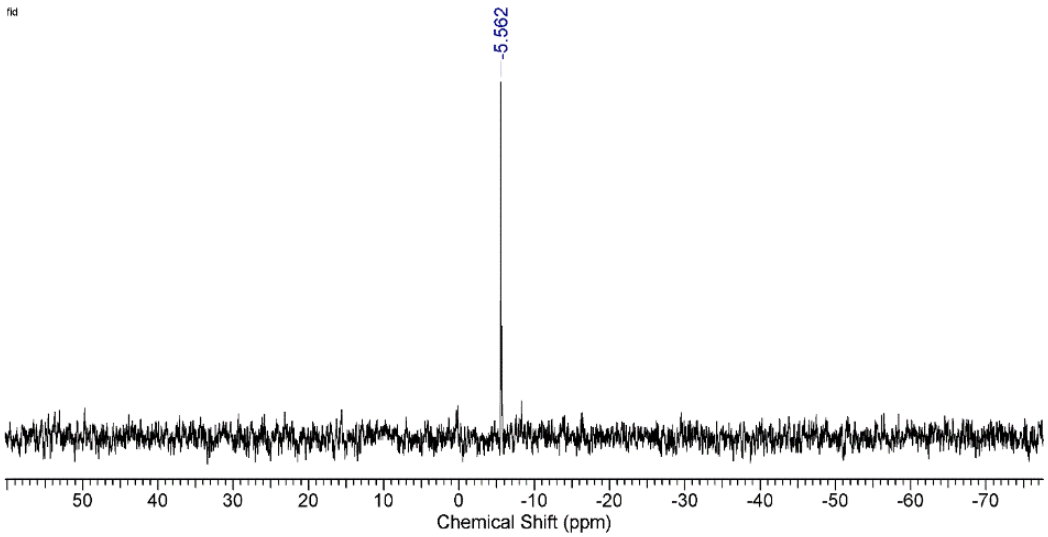

Figure S6. ^{119}Sn NMR spectrum of (p*S*)-**3**.

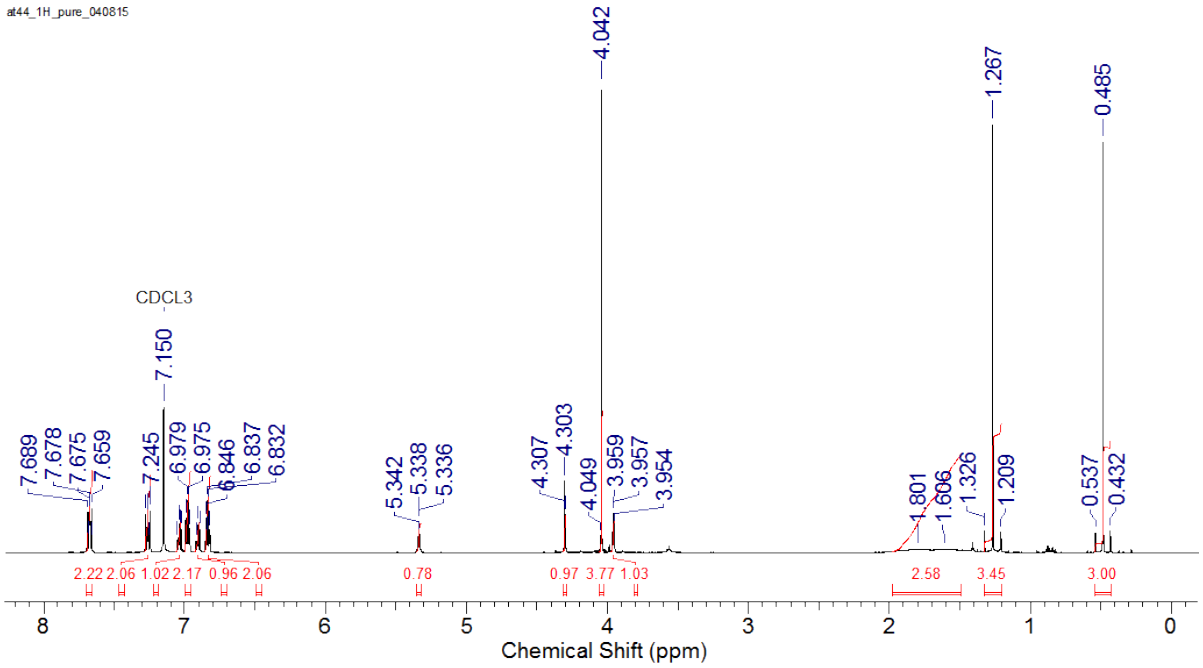

Figure S7a. ^{1}H NMR spectrum of (p*S*)-**4**.

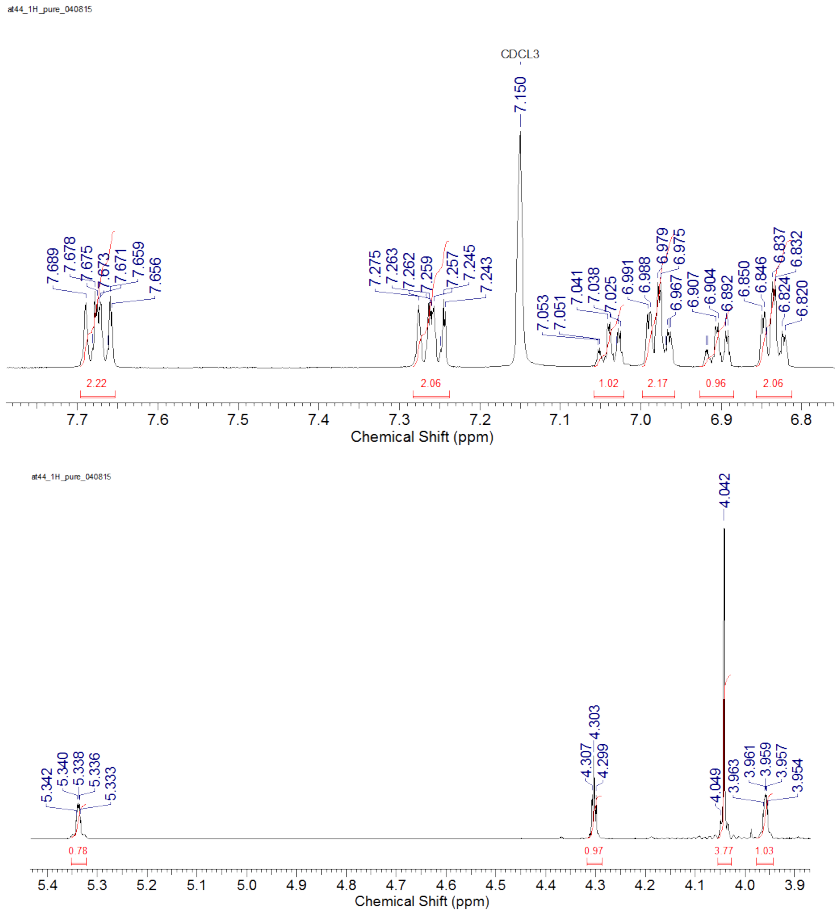

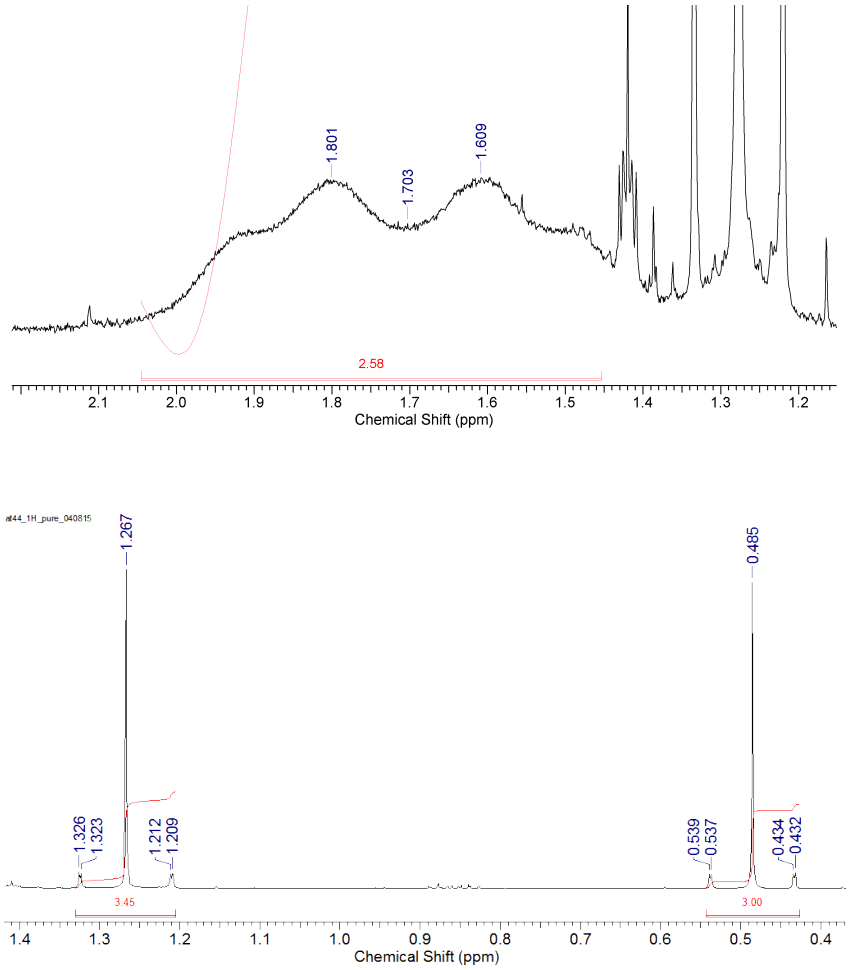

Figure S7b. Expansions of the ^{1}H NMR spectrum of (p*S*)-**4**.

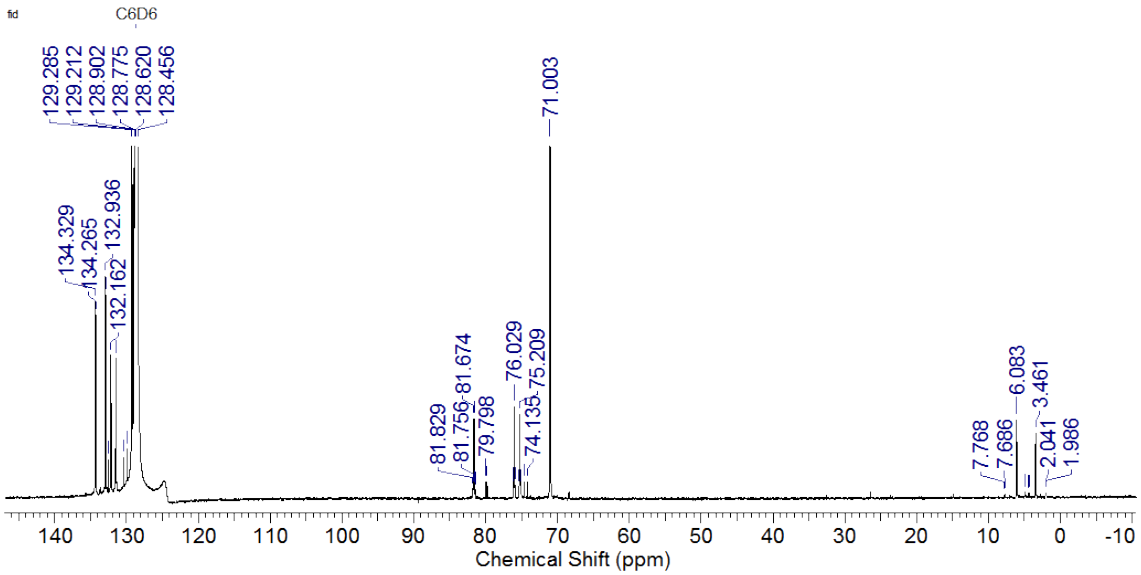

Figure S8a. ^{13}C NMR spectrum of (p*S*)-**4**.

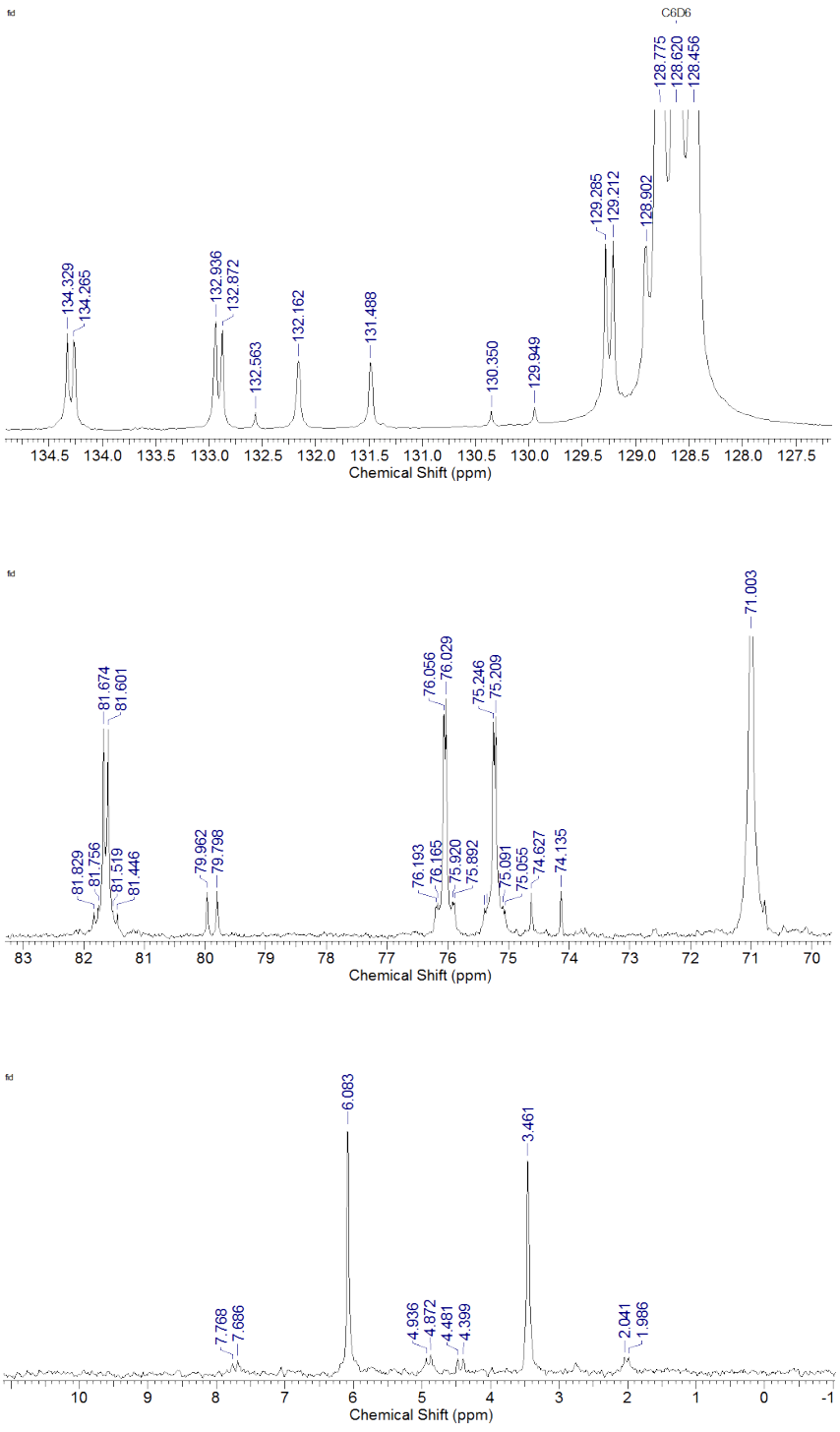

Figure S8b. Expansions of the ^{13}C NMR spectrum of (p*S*)-**4**.

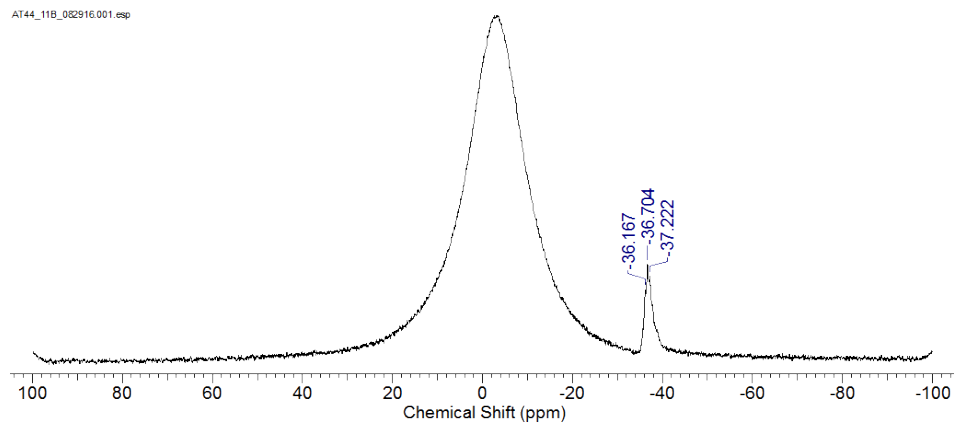

Figure S9. ^{11}B NMR spectrum of (p*S*)-**4**.

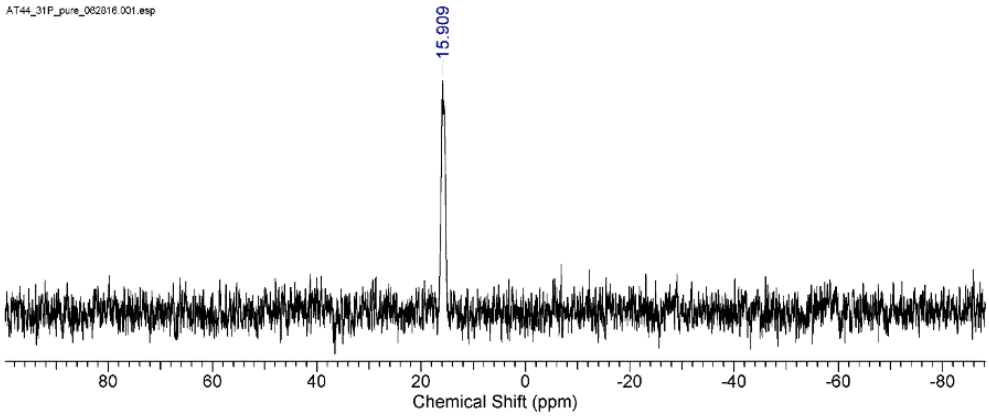

Figure S10. ^{31}P NMR spectrum of (p*S*)-**4**.

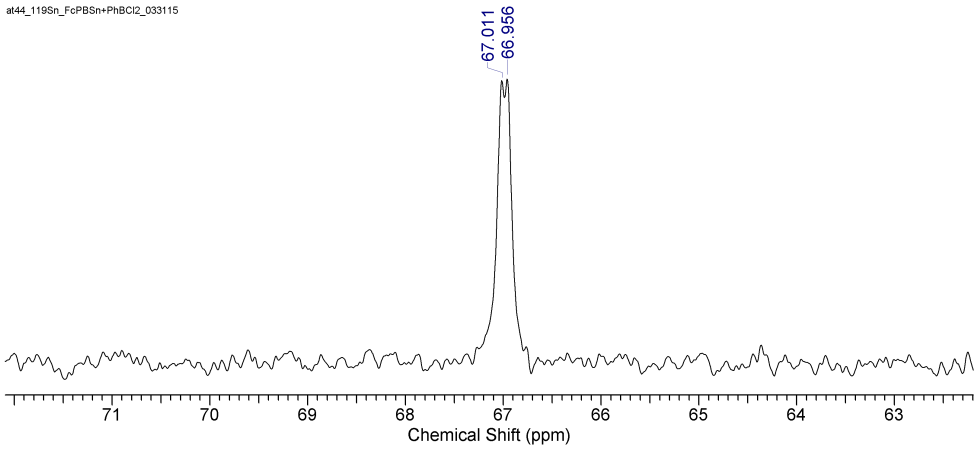

Figure S11. ^{119}Sn NMR spectrum of (p*S*)-**4**.

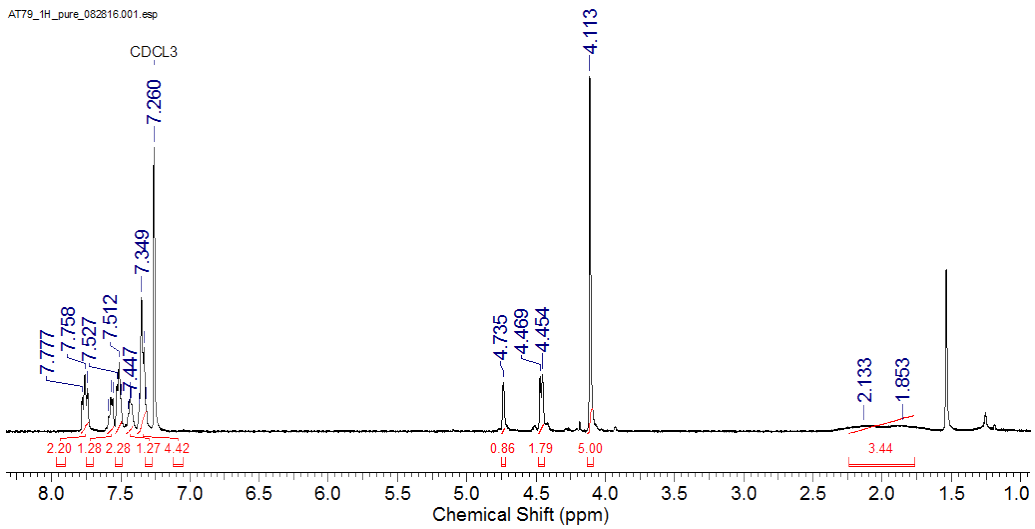

Figure S12a. ^{1}H NMR spectrum of *rac*-**5**.

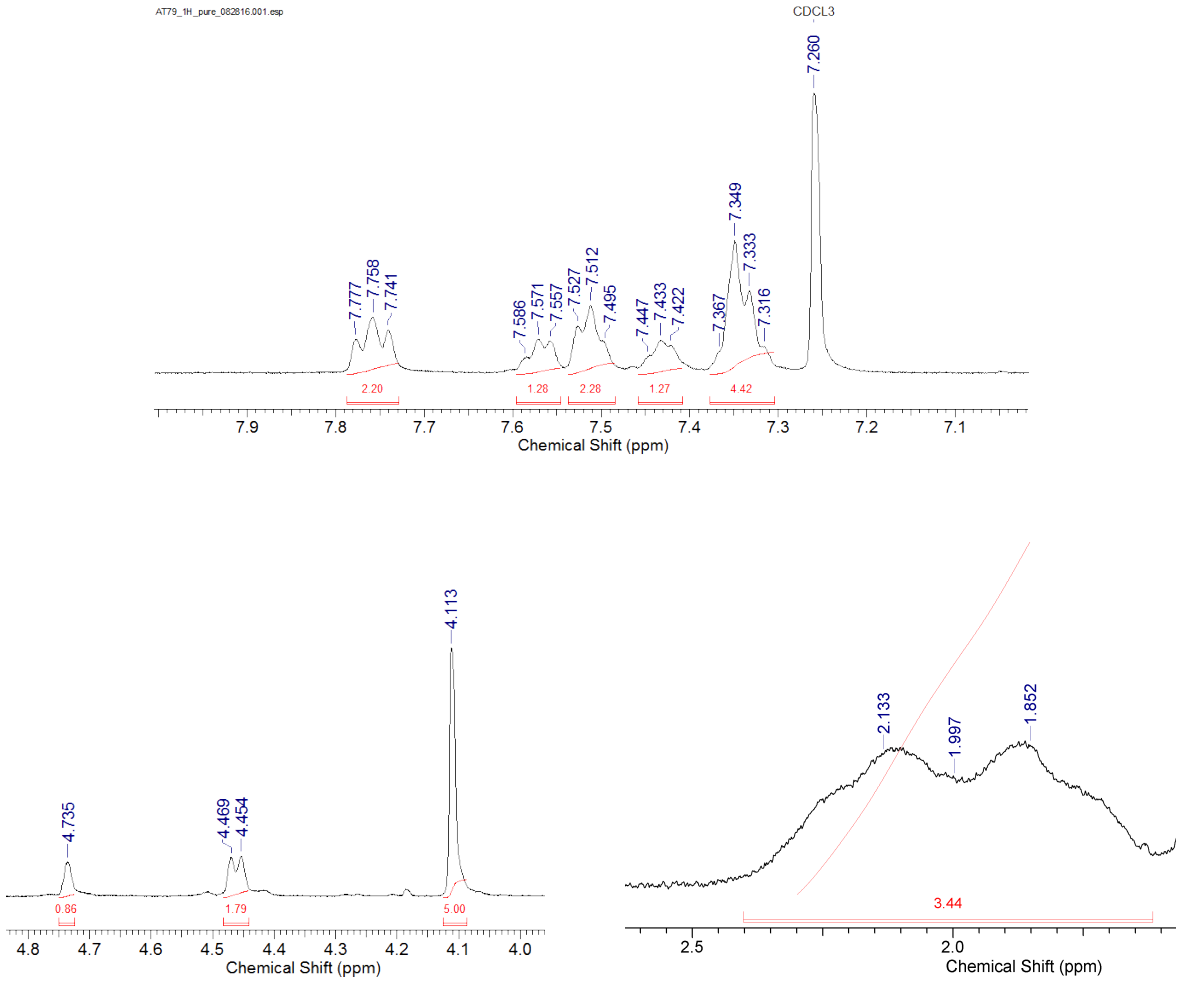

Figure S12b. Expansions of the ^{1}H NMR spectrum of *rac*-**5**.

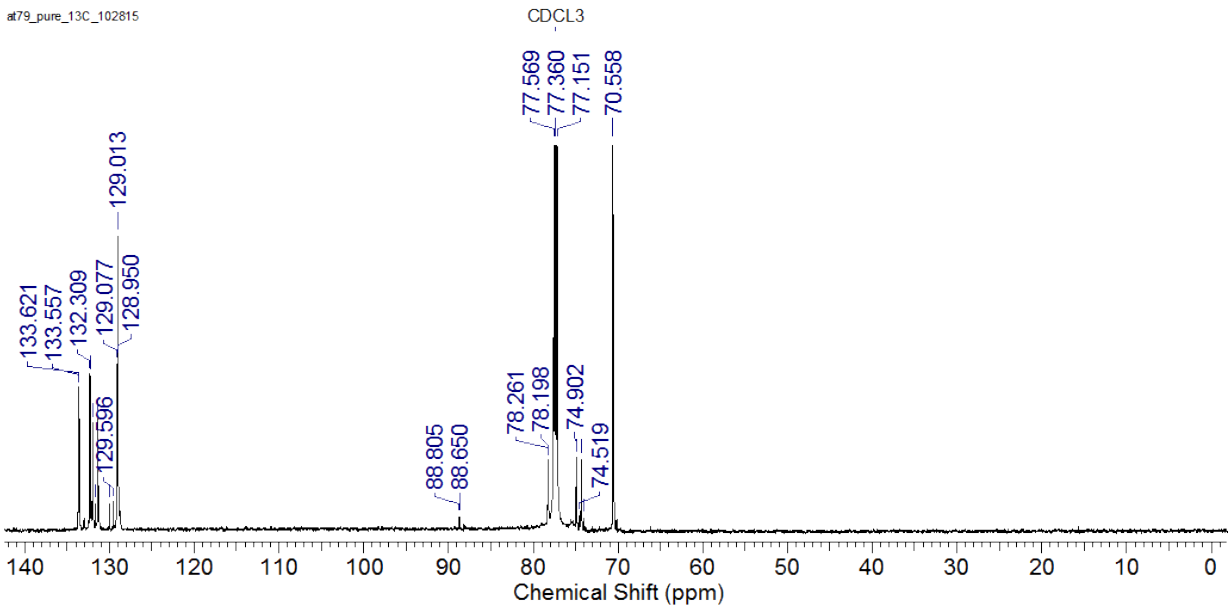

Figure S13a. ^{13}C NMR spectrum of *rac*-**5**.

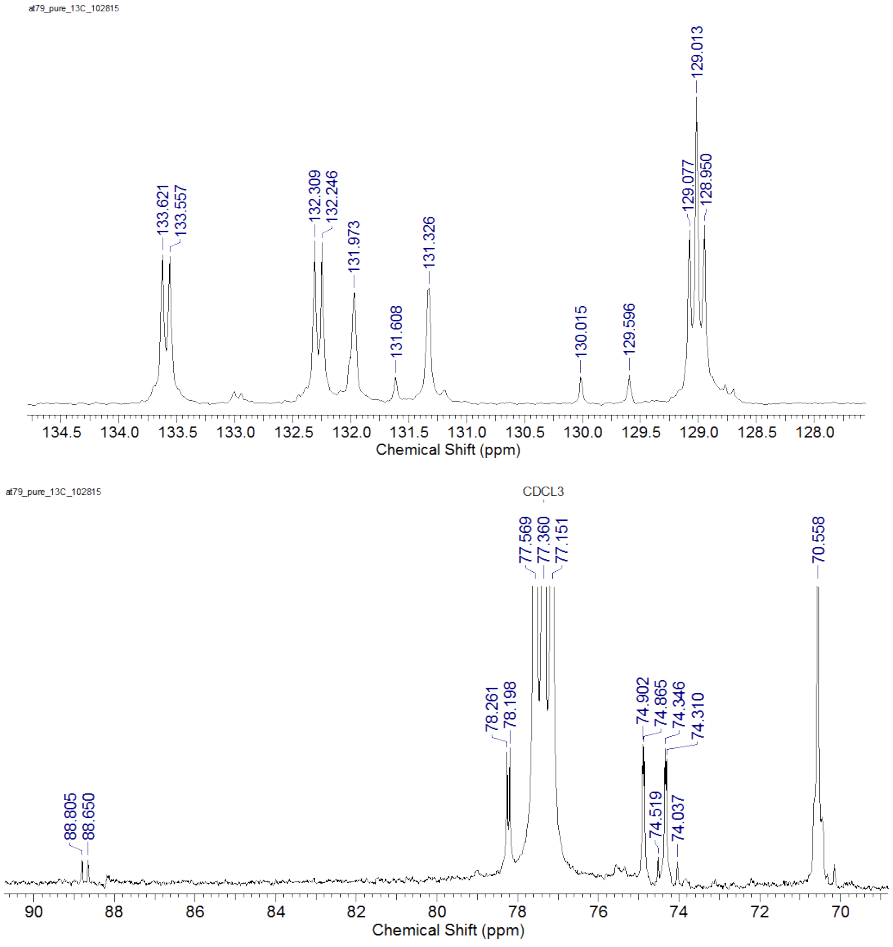

Figure S13b. Expansions of the ^{13}C NMR spectrum of *rac*-**5**.

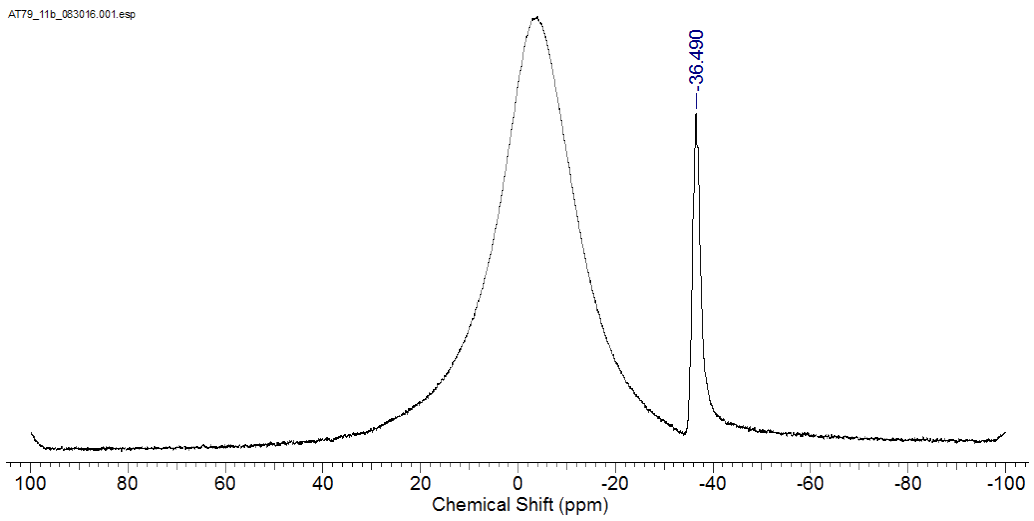

Figure S14. ^{11}B NMR spectrum of *rac*-**5**.

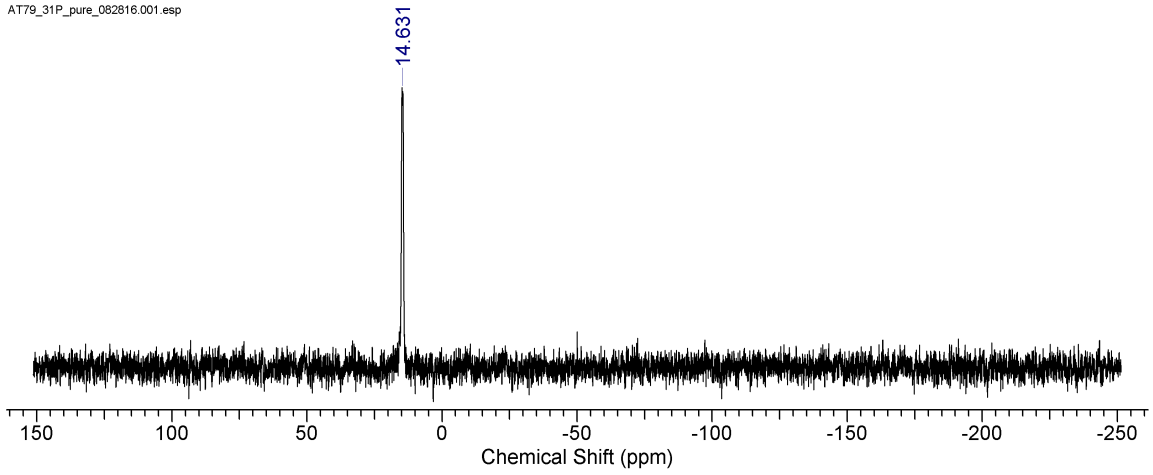

Figure S15. ^{31}P NMR spectrum of *rac*-**5**.

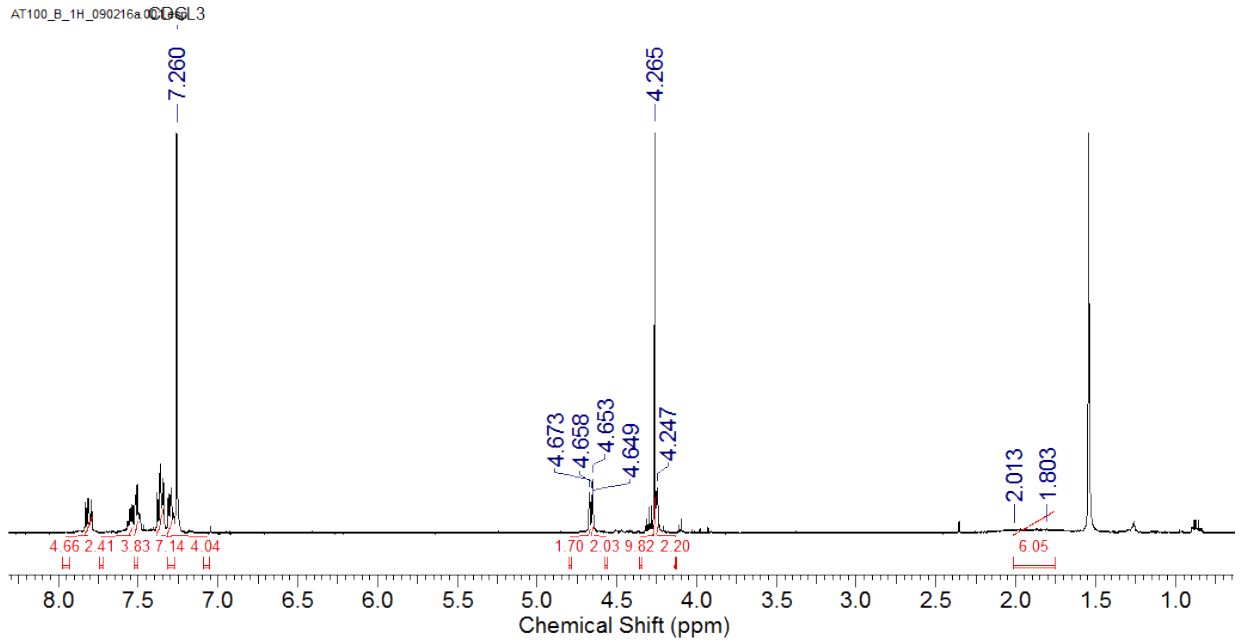

Figure S16a. ^{1}H NMR spectrum of (p*S*p*S*)-**6**.

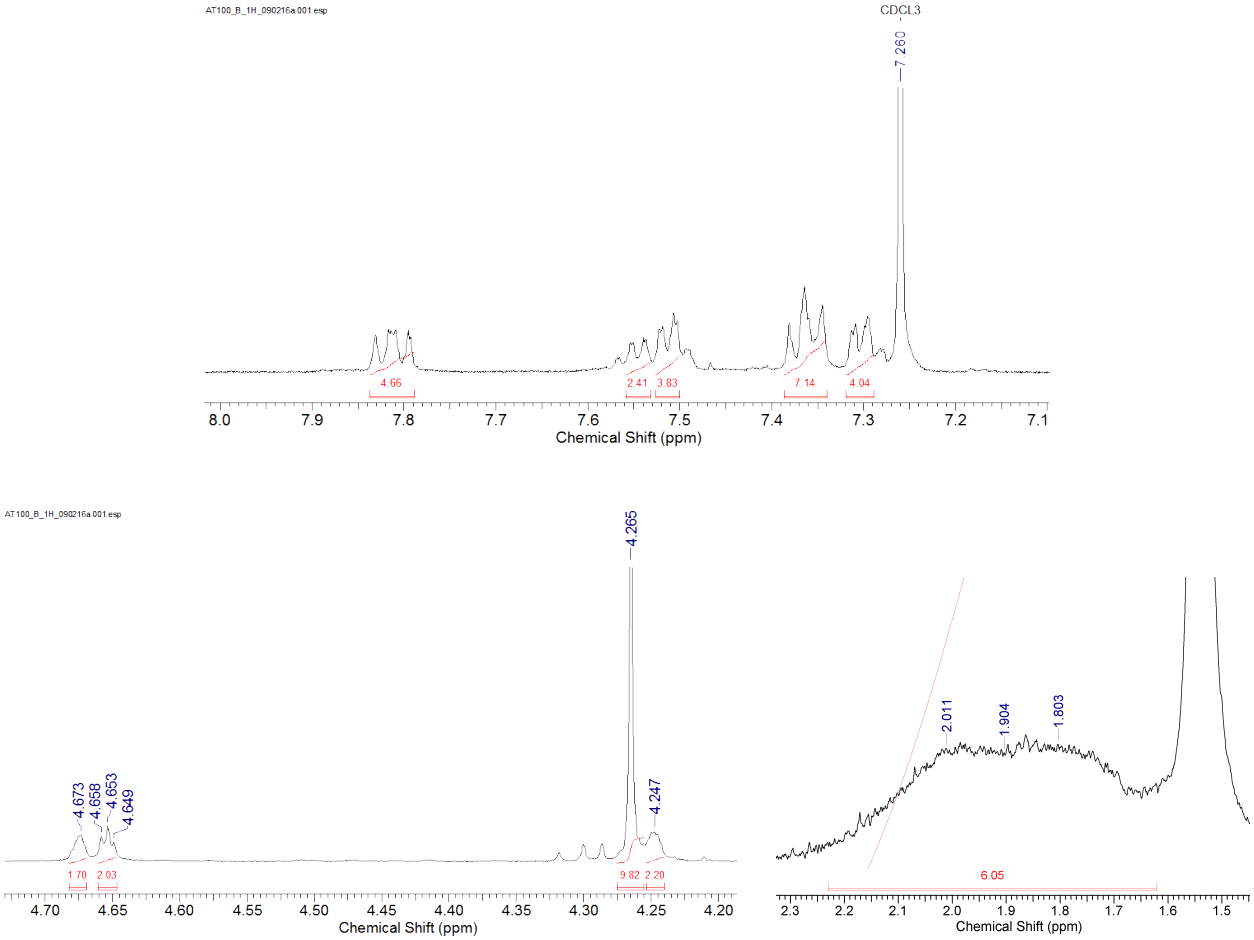

Figure S16b. Expansions of the ^{1}H NMR spectrum of (p*S*p*S*)-**6**.

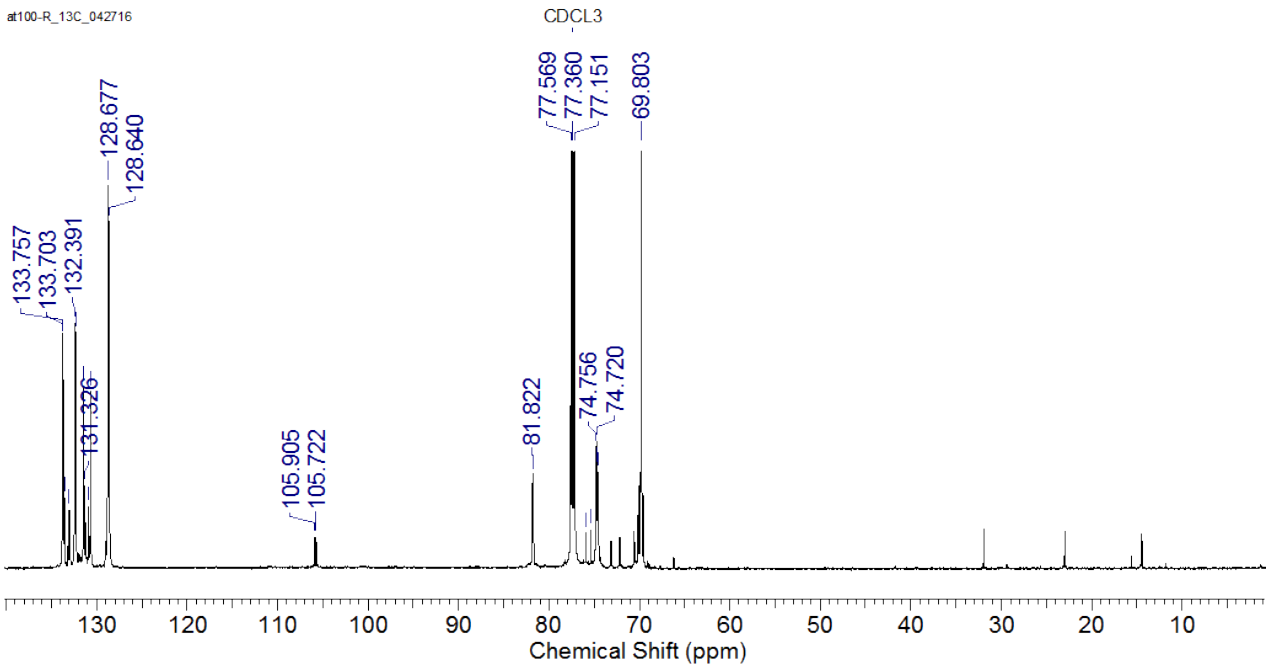

Figure S17a. ^{13}C NMR spectrum of (p*S*p*S*)-**6**.

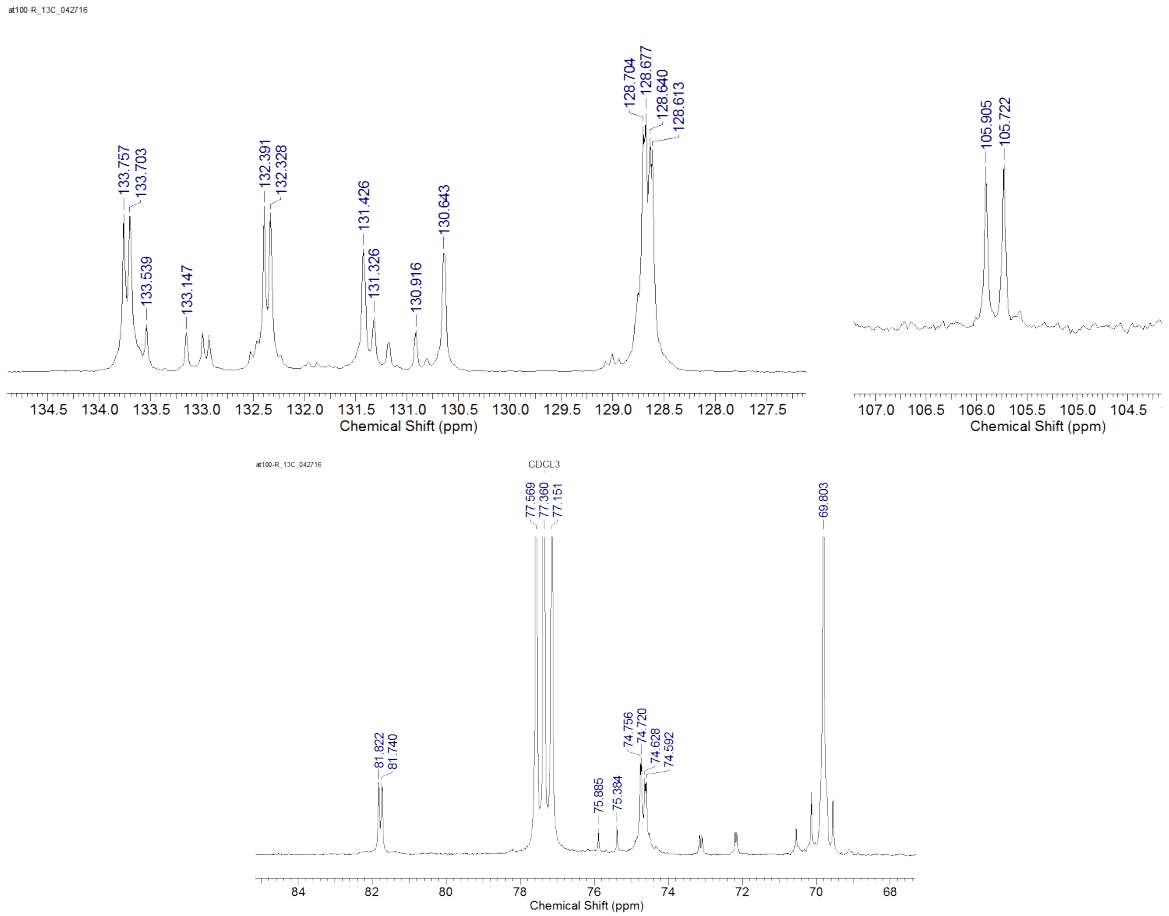

Figure S17b. Expansions of the ^{13}C NMR spectrum of (p*S*p*S*)-**6**.

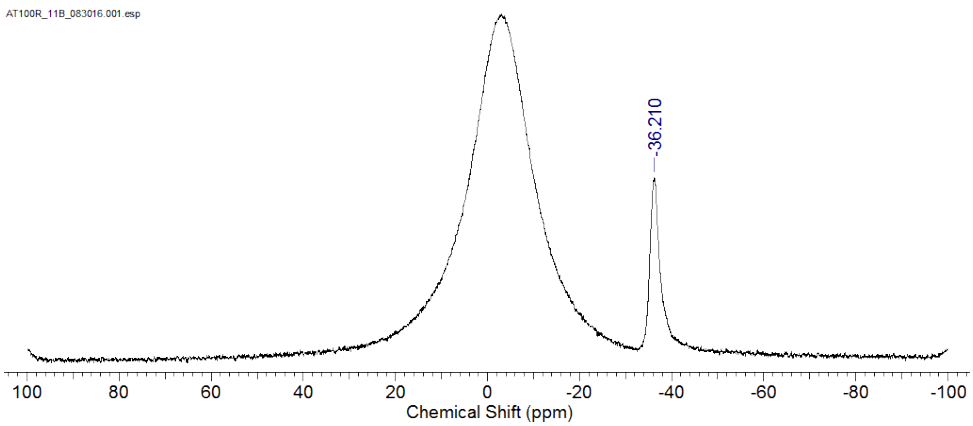

Figure S18. ^{11}B NMR spectrum of (p*S*p*S*)-**6**.

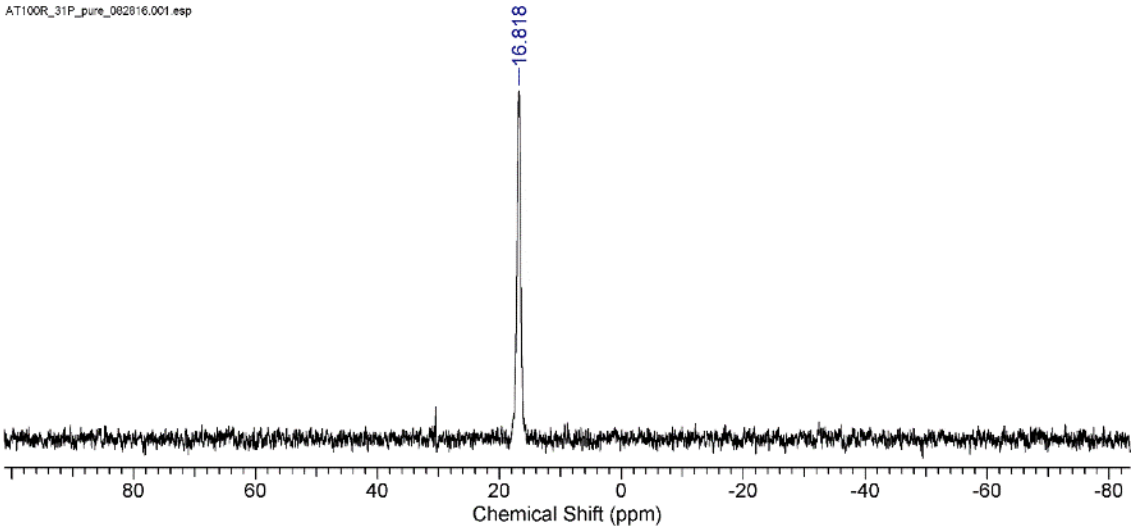

Figure S19. ^{31}P NMR spectrum of (p*S*p*S*)-**6**.

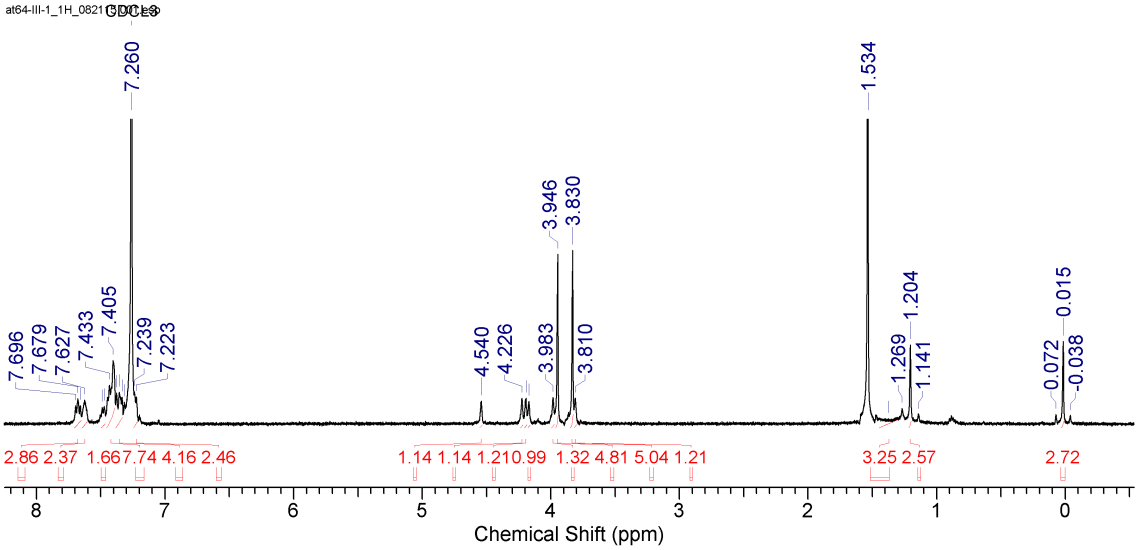

Figure S20a. ^{1}H NMR spectrum of (p*S*p*S*)-**7**.

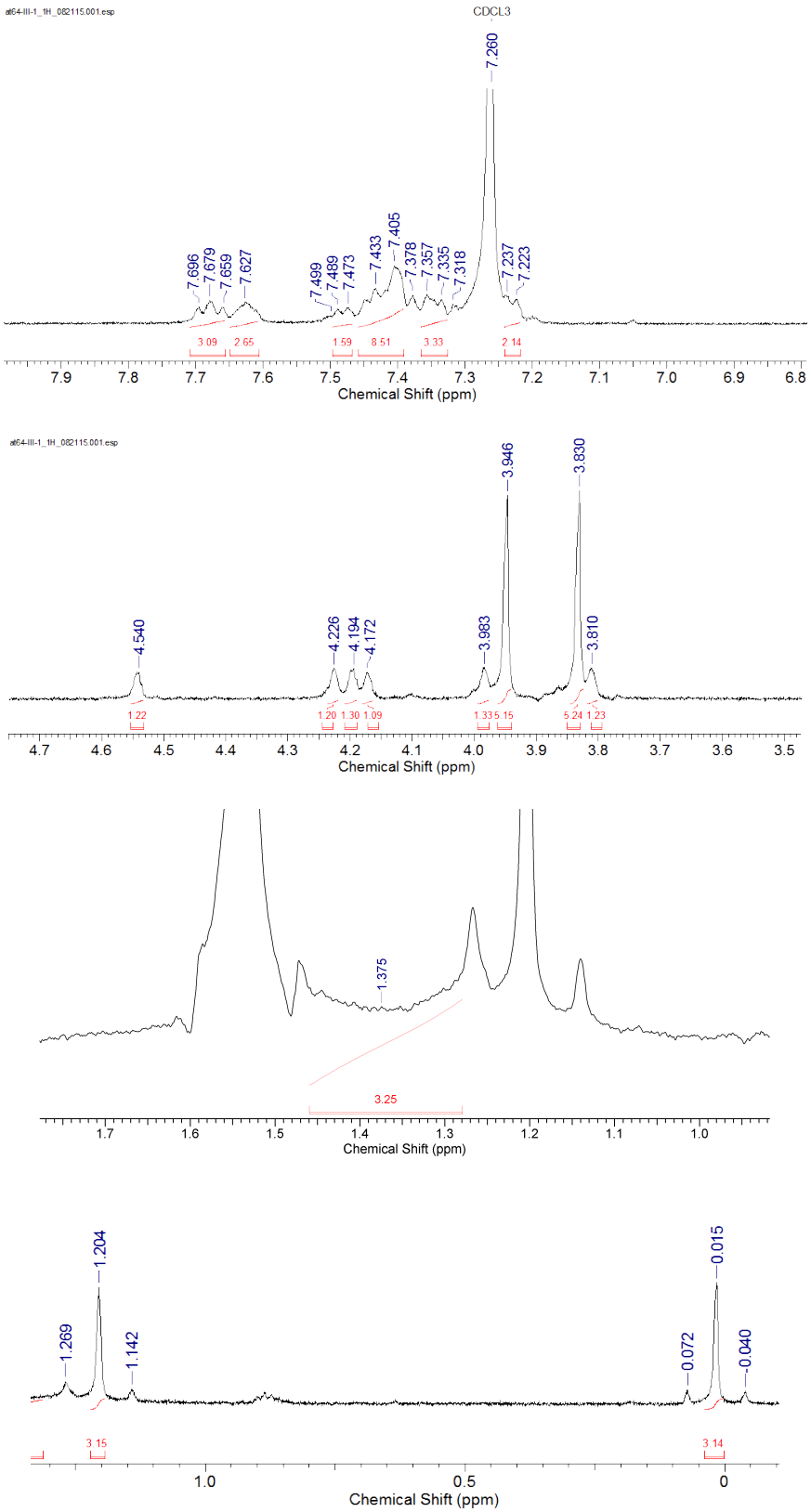

Figure S20b. Expansions of the ^{1}H NMR spectrum of (p*S*p*S*)-**7**.

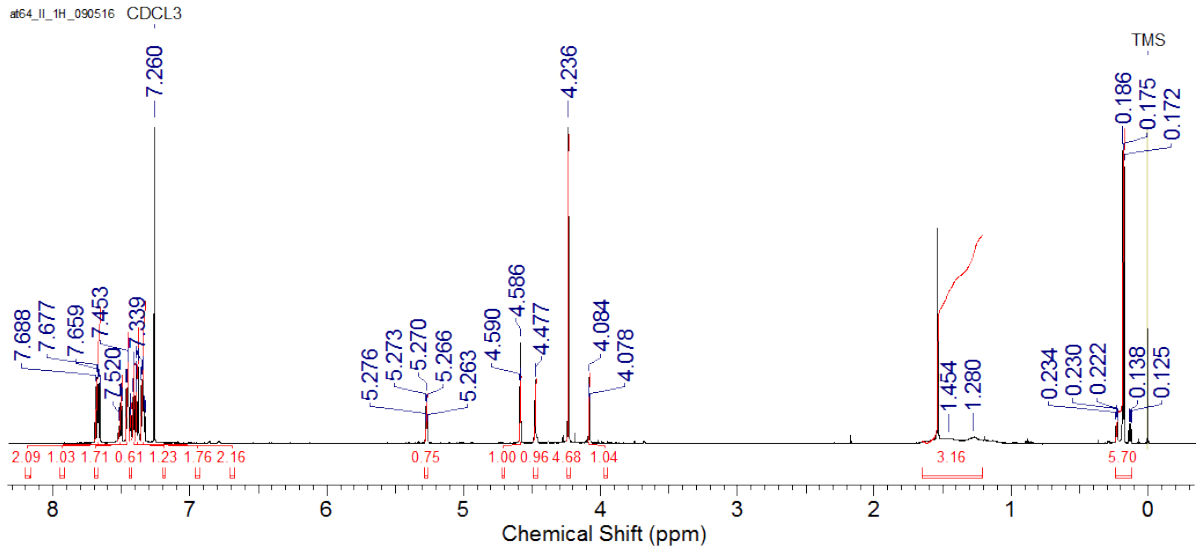

Figure S21a. ^{1}H NMR spectrum of (p*S*)-**8**.

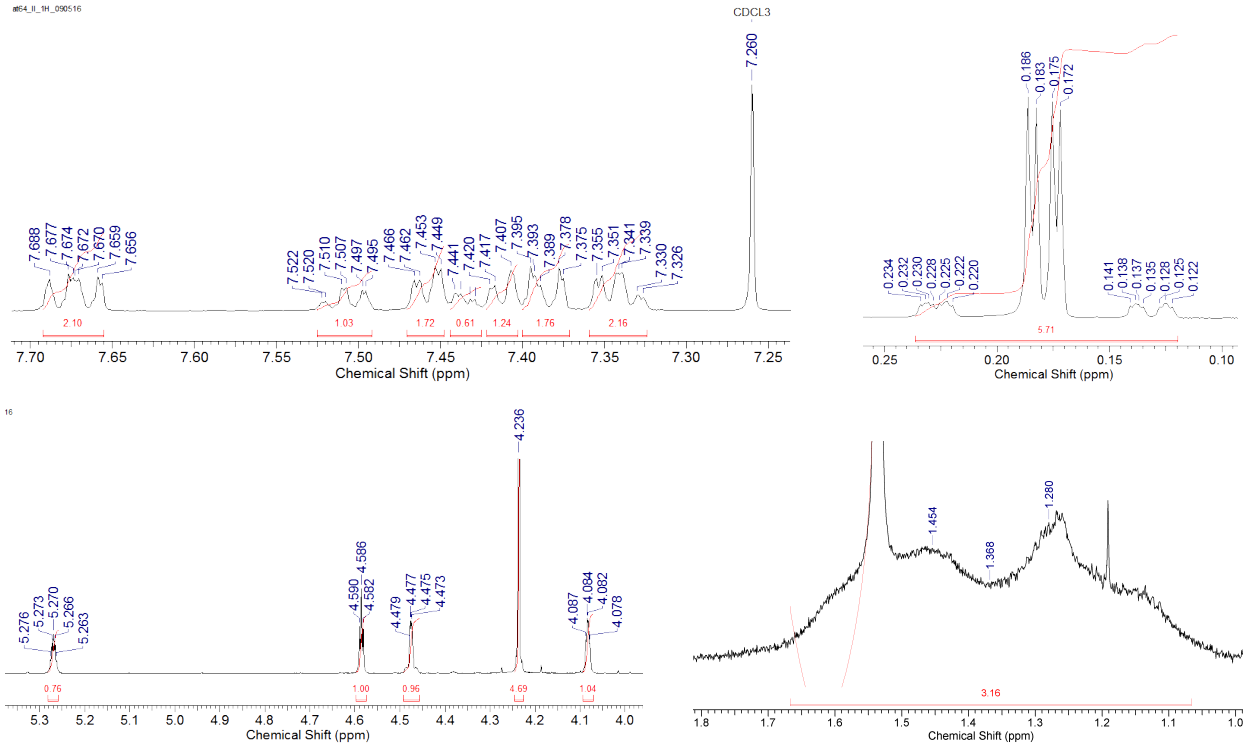

Figure S21b. Expansions of the ^{1}H NMR spectrum of (p*S*)-**8**.

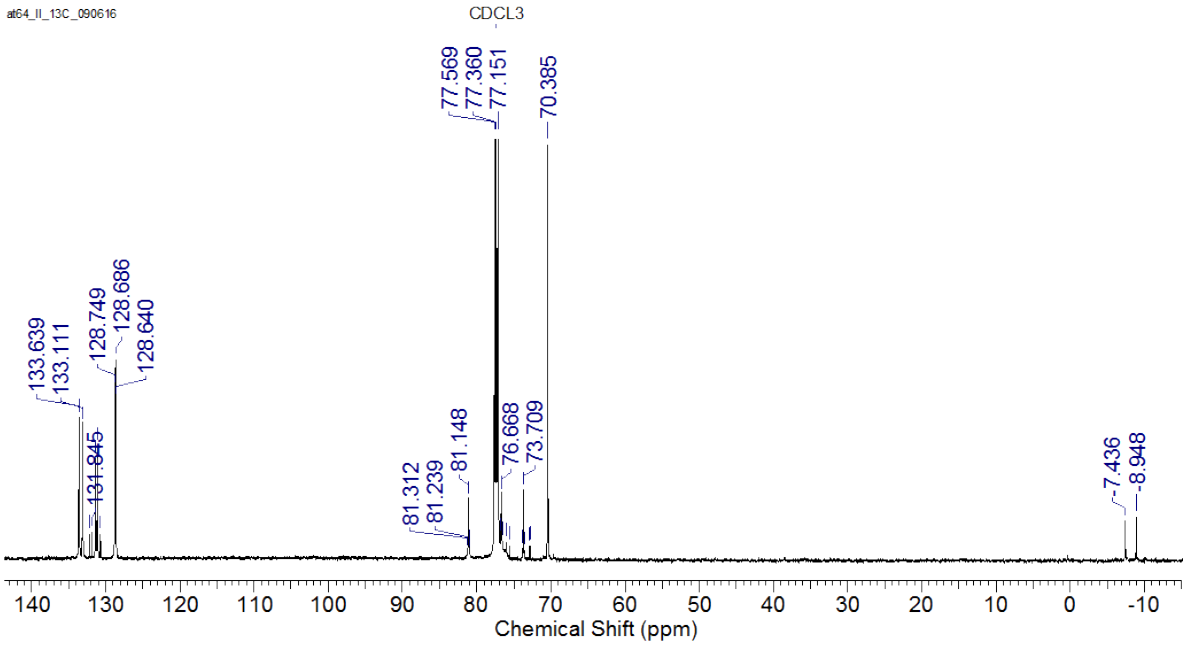

Figure S22a. ^{13}C NMR spectrum of (p*S*)-**8**.

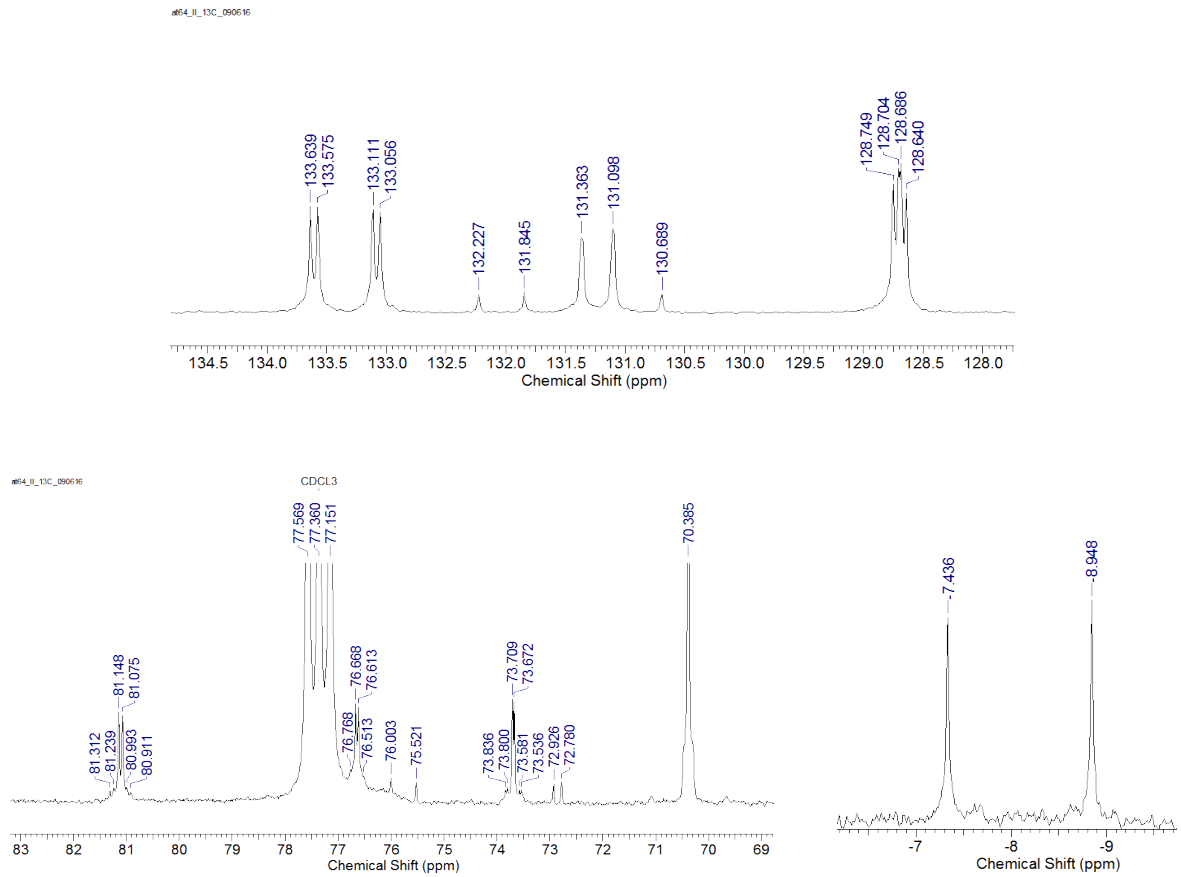

Figure S22b. Expansions of the ^{13}C NMR spectrum of (p*S*)-**8**.

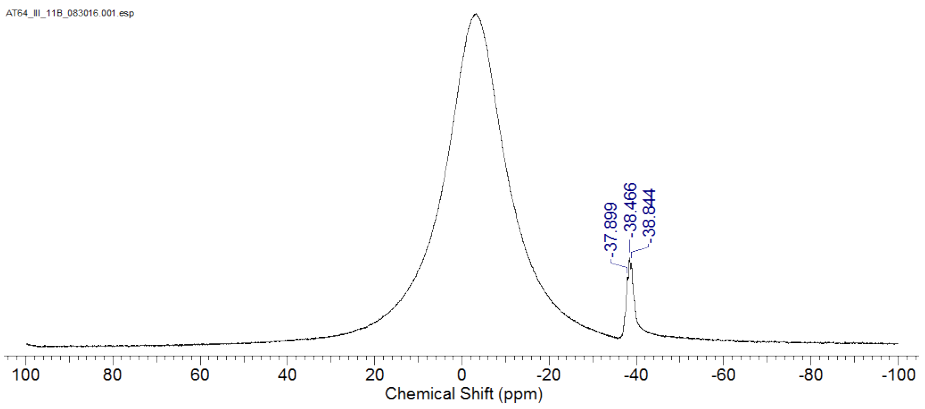

Figure S23. ^{11}B NMR spectrum of (p*S*)-**8**.

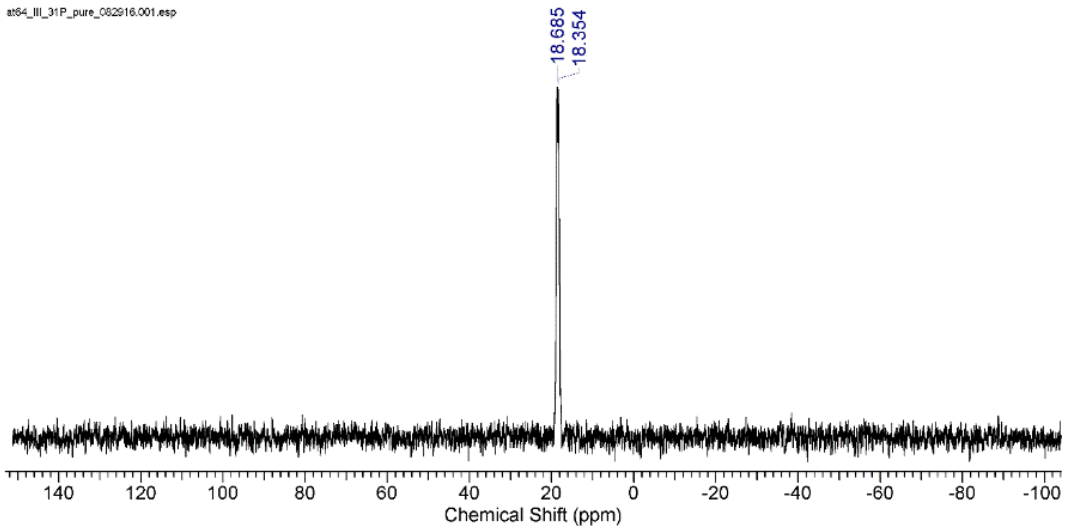

Figure S24. ^{31}P NMR spectrum of (p*S*)-**8**.

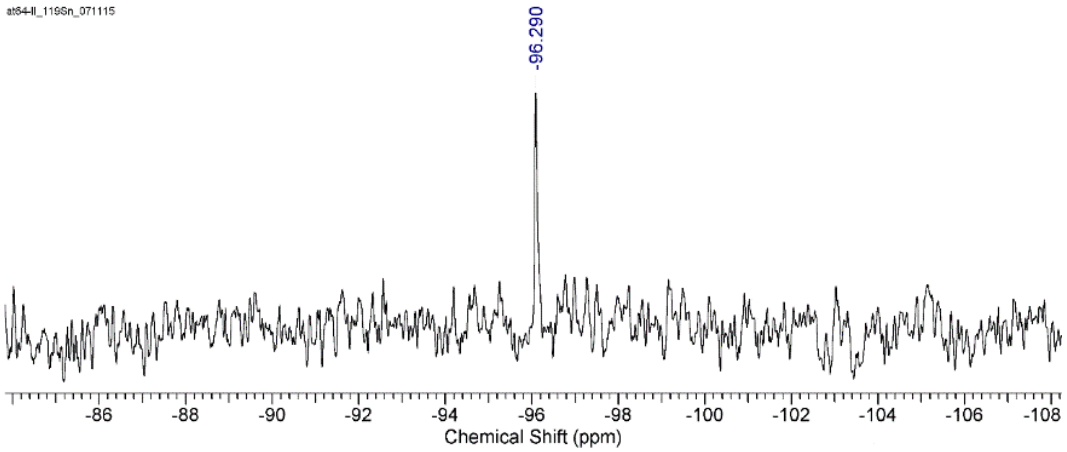

Figure S25. ^{119}Sn NMR spectrum of (p*S*)-**8.**

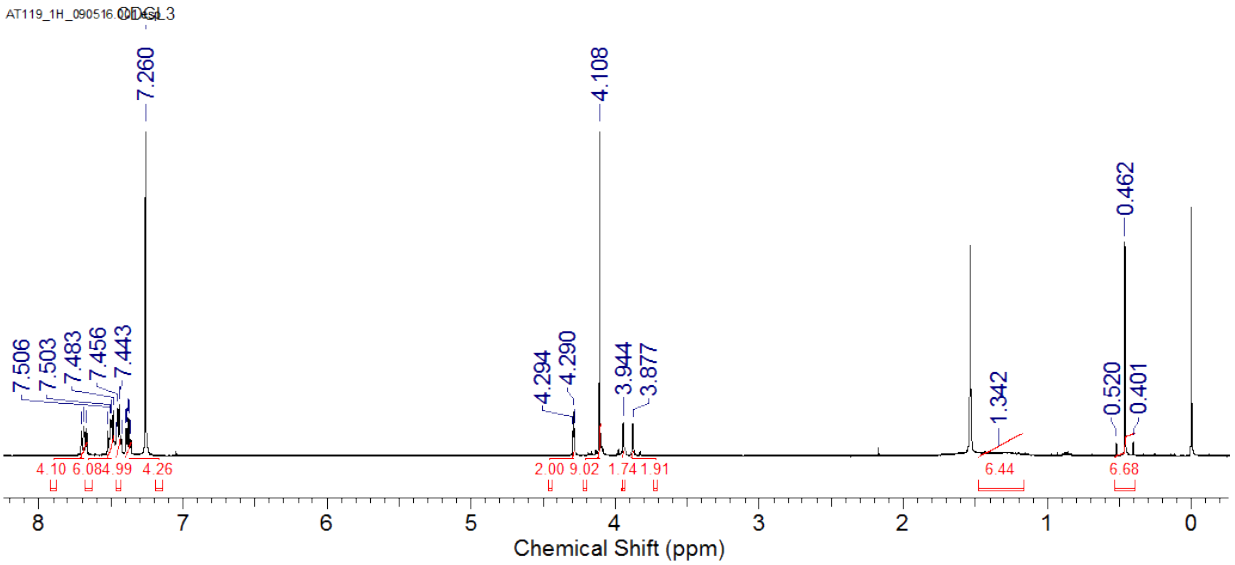

Figure S26a. ^{1}H NMR spectrum of (p*R*p*R*)-**10**.

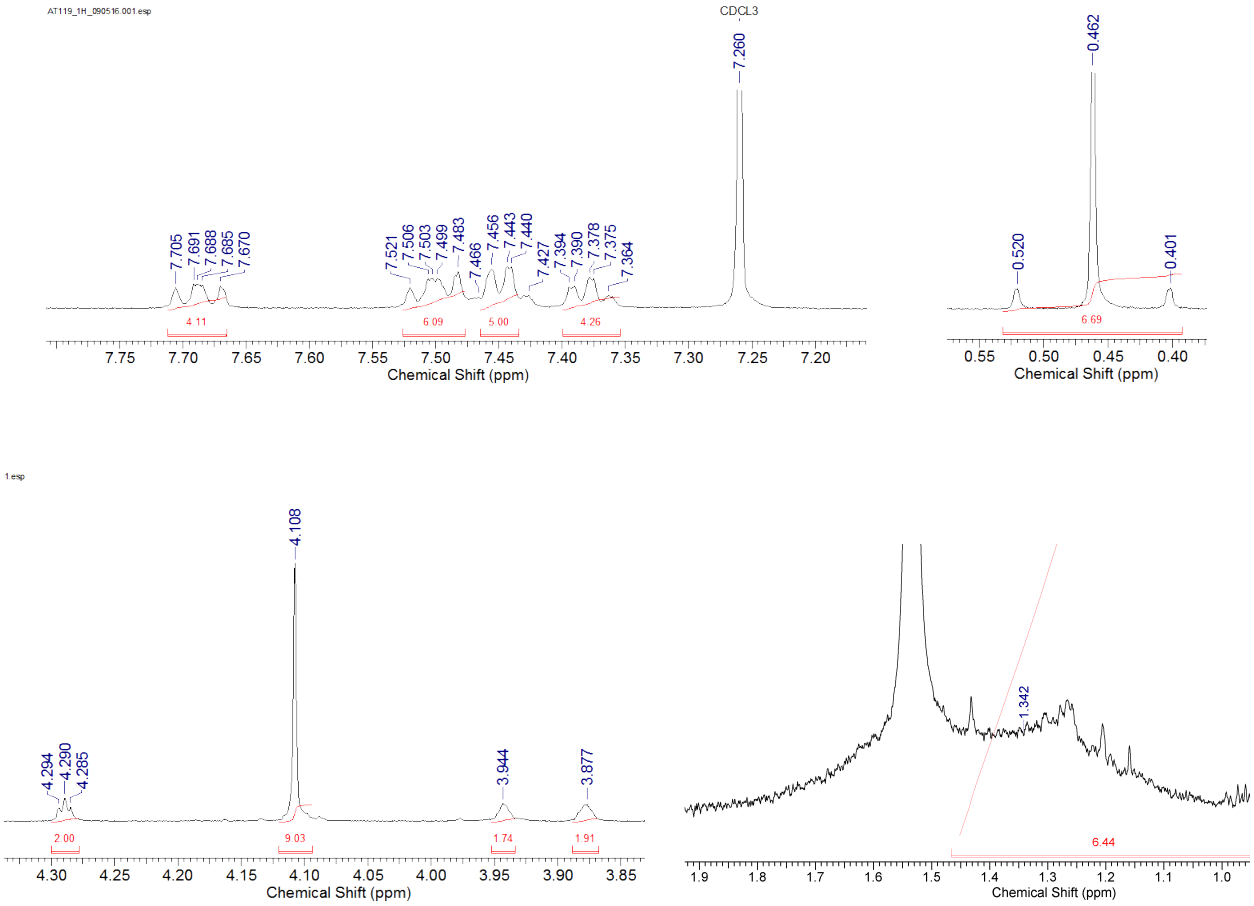

Figure S26b. Expansions of the ^{1}H NMR spectrum of (p*R*p*R*)-**10**.

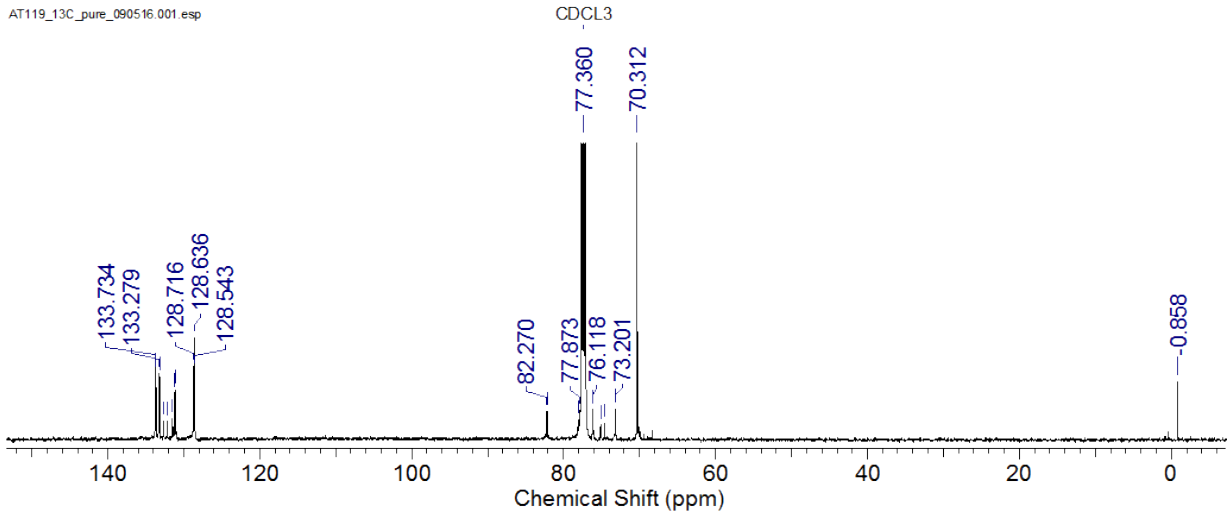

Figure S27a. ^{13}C NMR spectrum of (p*R*p*R*)-**10**.

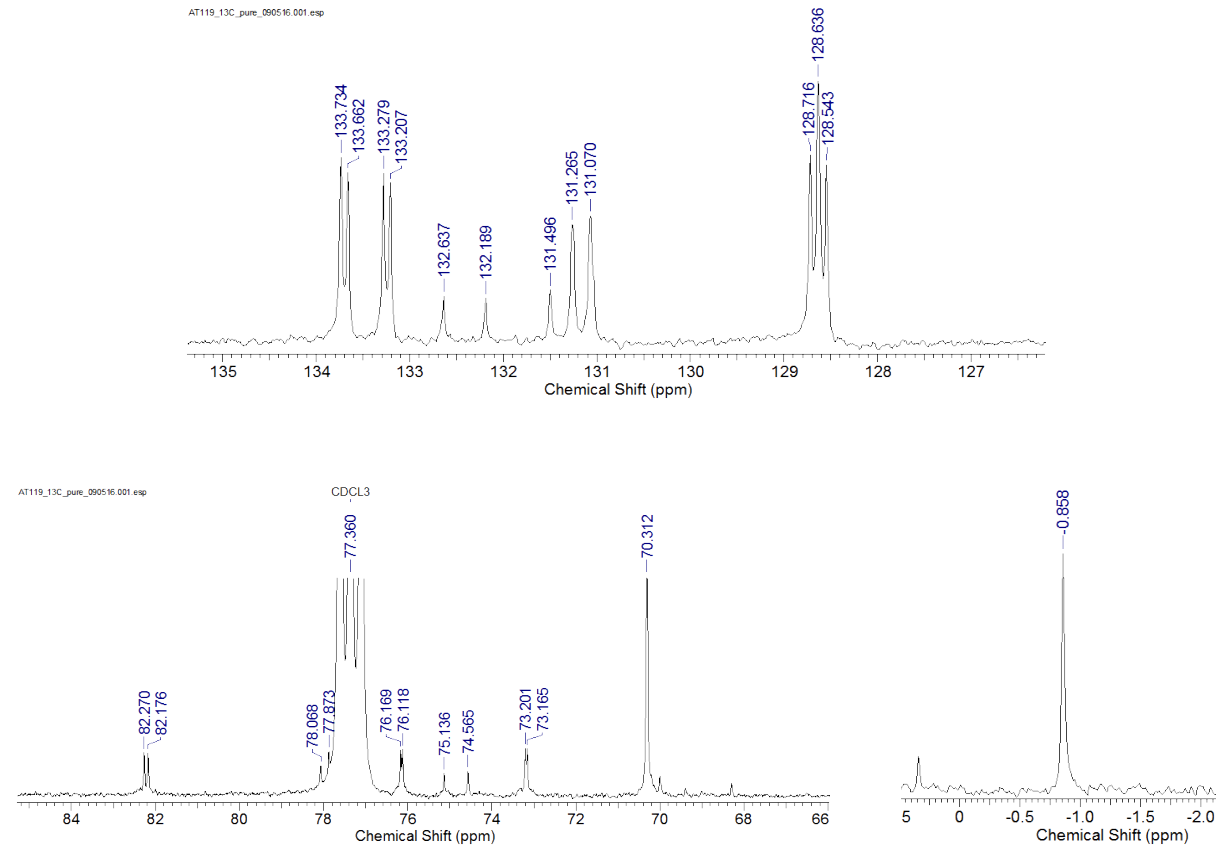

Figure S27b. Expansions of the ^{13}C NMR spectrum of (p*R*p*R*)-**10**.

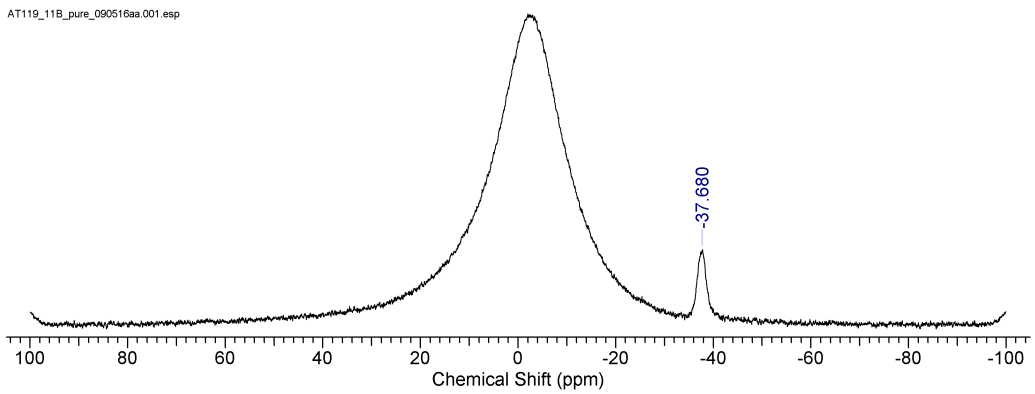

Figure S28. ^{11}B NMR spectrum of (p*R*p*R*)-**10**.

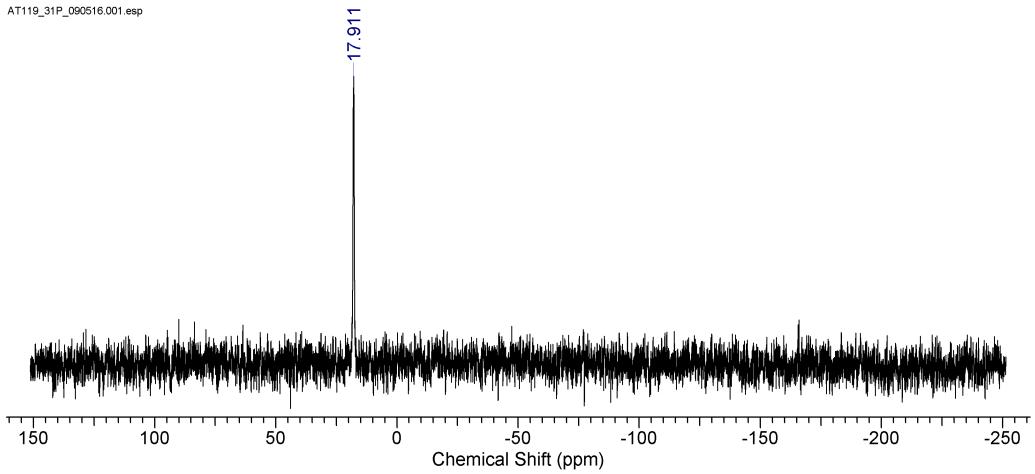

Figure S29. ^{31}P NMR spectrum of (p*R*p*R*)-**10**.

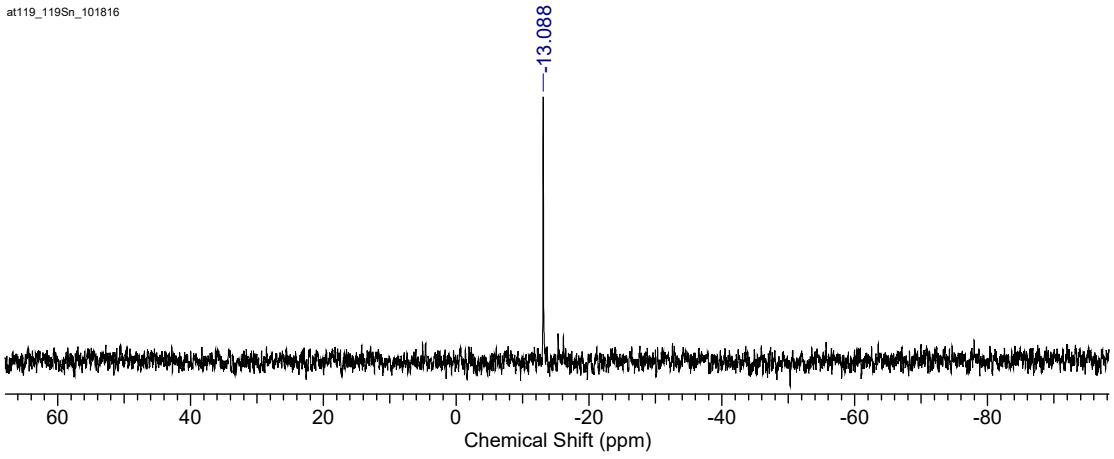

Figure S30. ^{119}Sn NMR spectrum of (p*R*p*R*)-**10**.

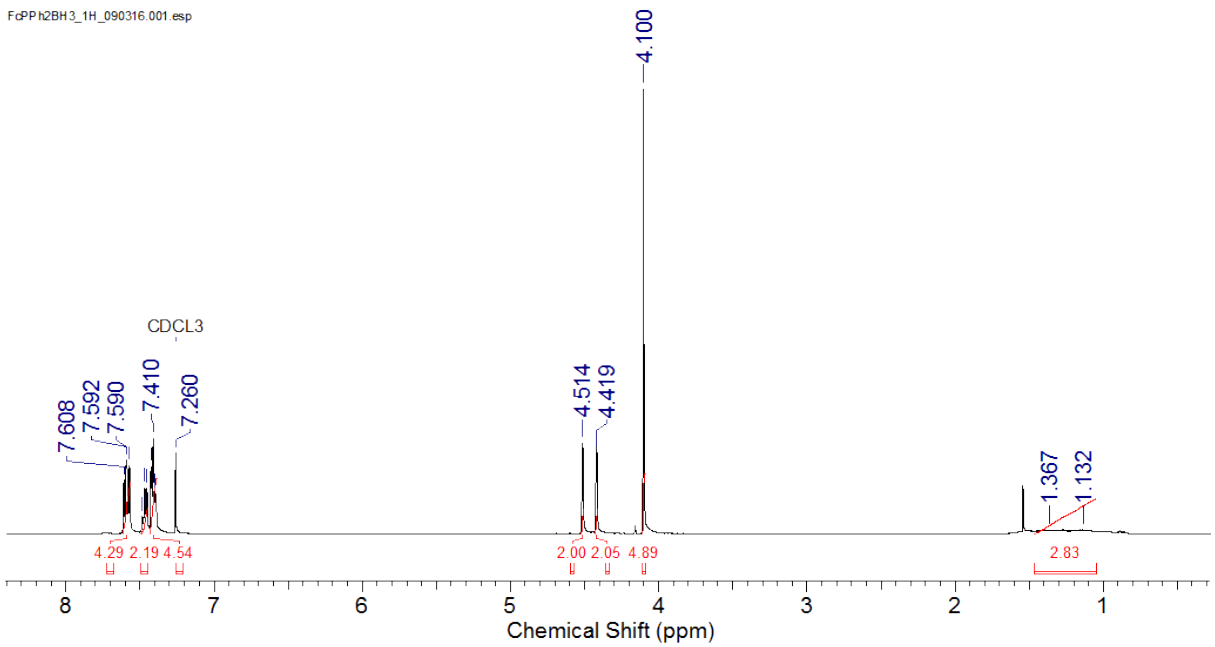

Figure S31a. ^{1}H NMR spectrum of **$FcPPh_2 \cdot BH_3$**.

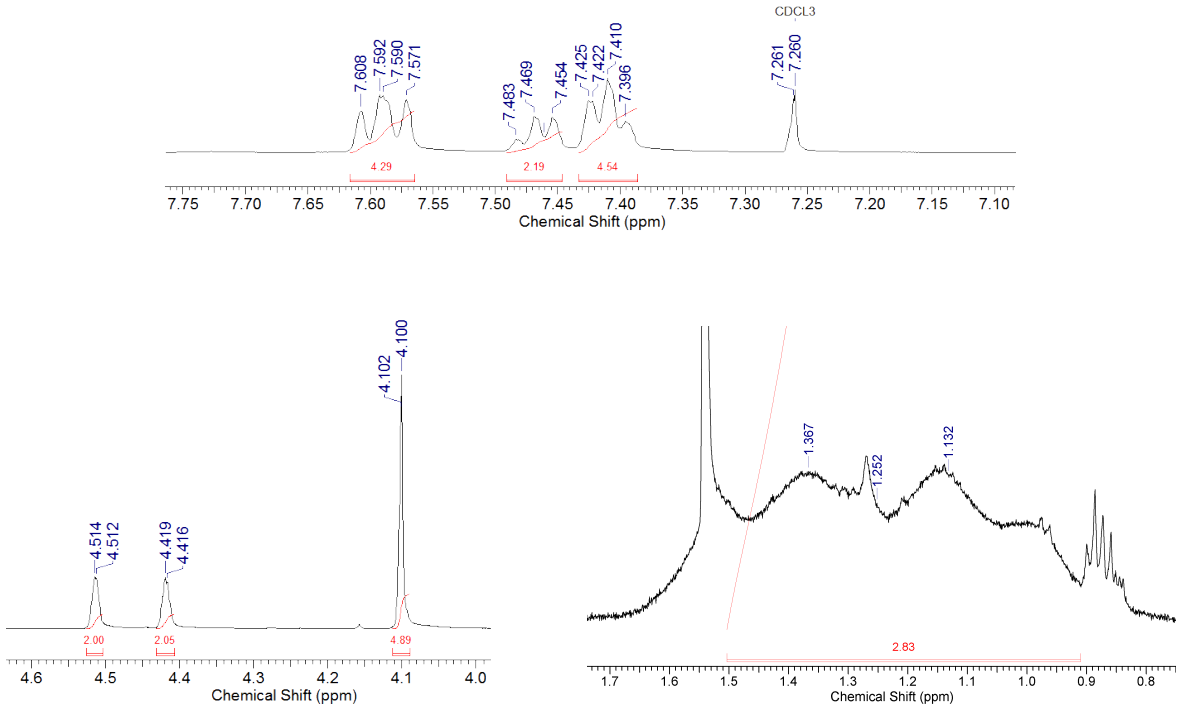

Figure S31b. Expansions of the ^{1}H NMR spectrum of **$FcPPh_2 \cdot BH_3$**.

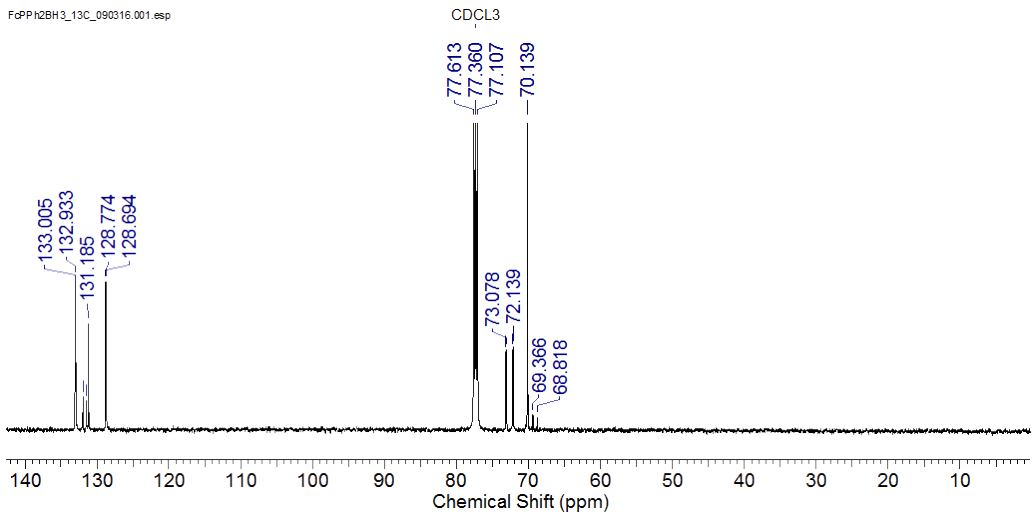

Figure S32a. ^{13}C NMR spectrum of **$FcPPh_2 \cdot BH_3$**.

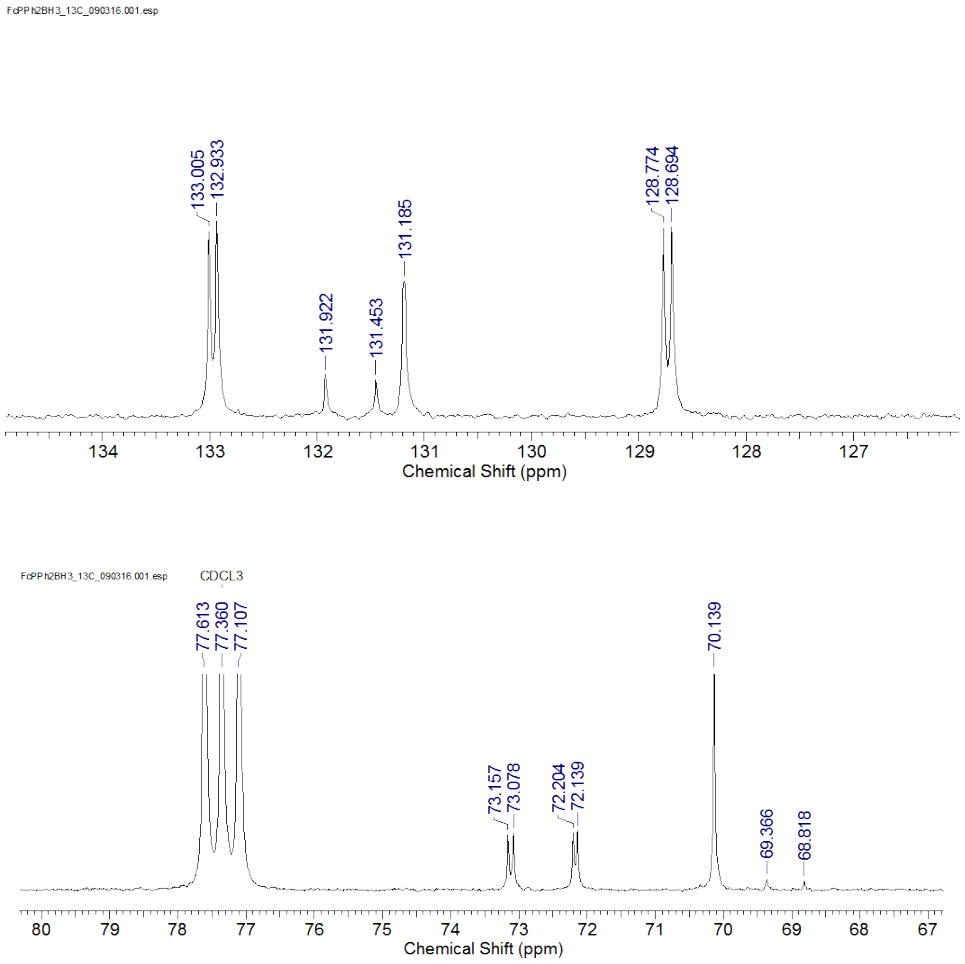

Figure S32b. Expansions of the ^{13}C NMR spectrum of **$FcPPh_2 \cdot BH_3$**.

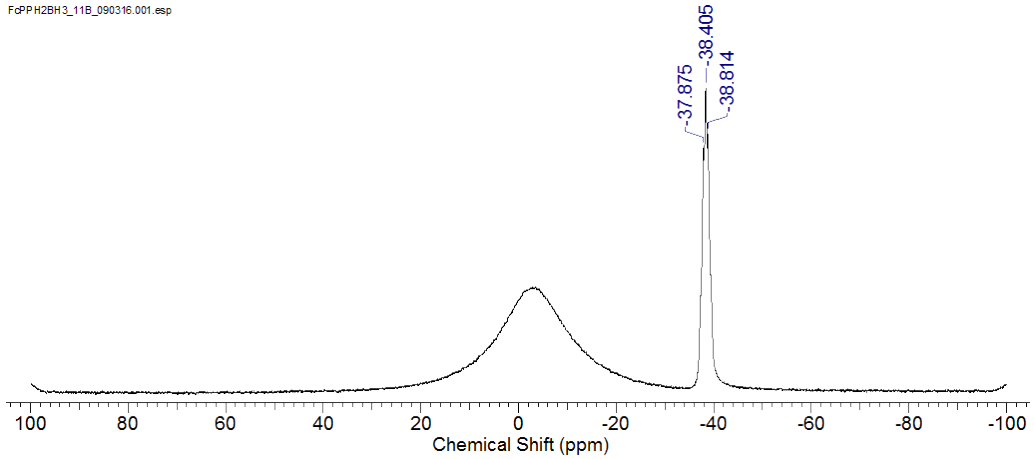

Figure S33. ^{11}B NMR spectrum of **FcPPh$_2$·BH$_3$**.

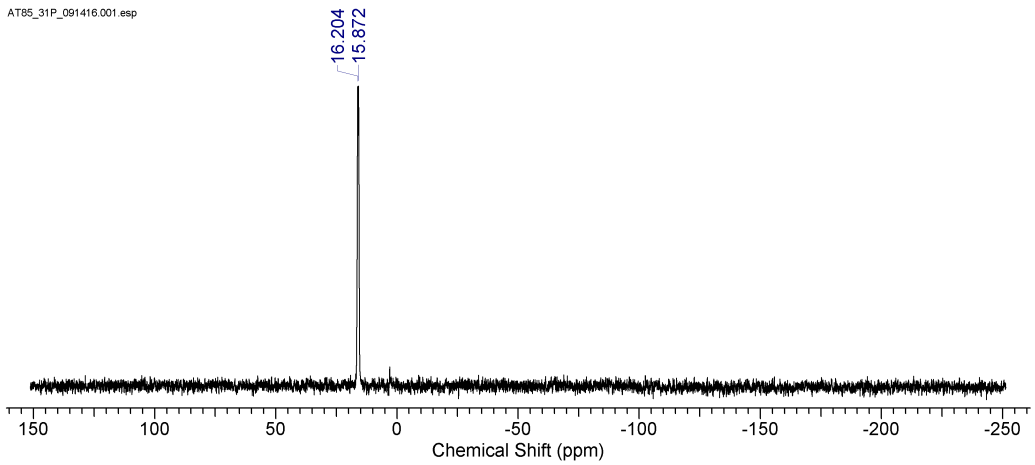

Figure S34. ^{31}P NMR spectrum of **FcPPh$_2$·BH$_3$**.

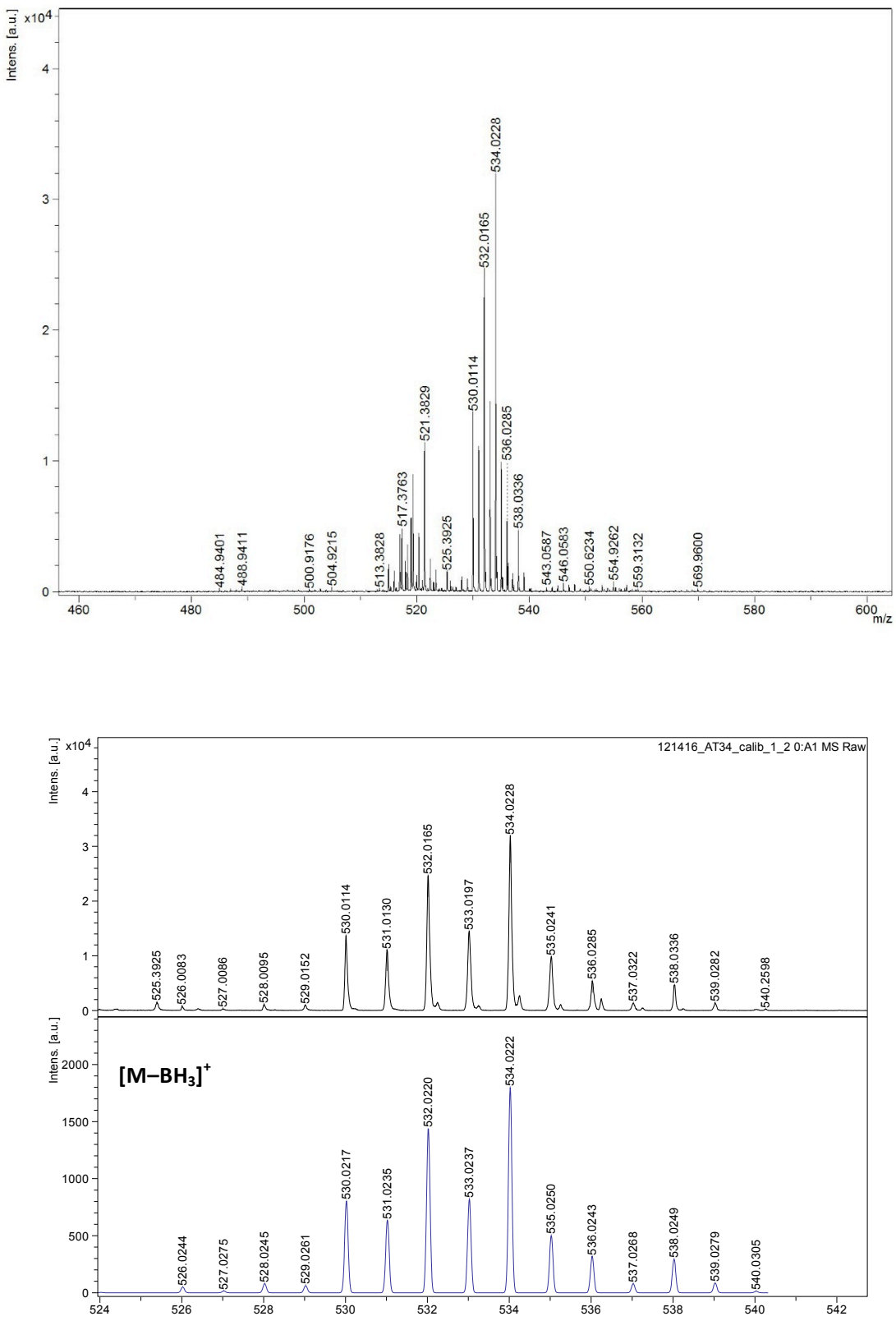

Figure S35. MALDI-TOF mass spectrum of (p*S*)-**3**.

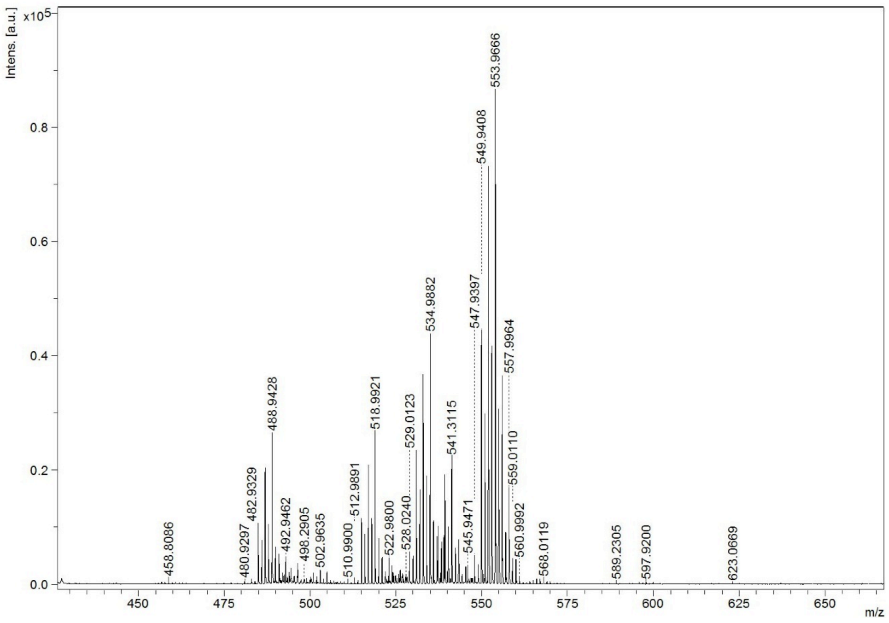

[M]$^+$

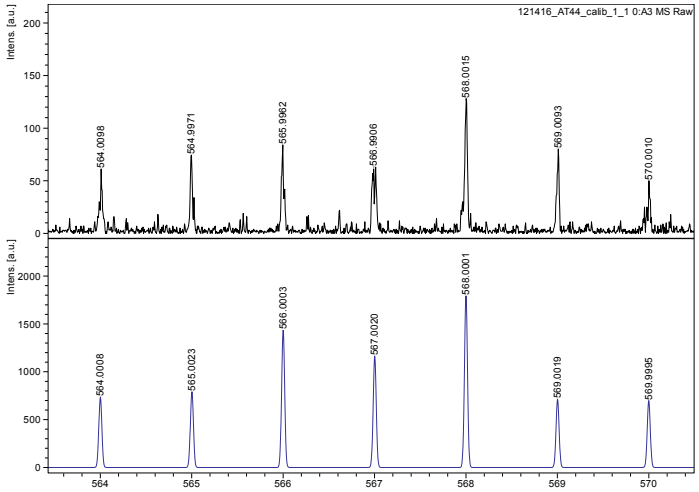

[M–BH$_3$]$^+$

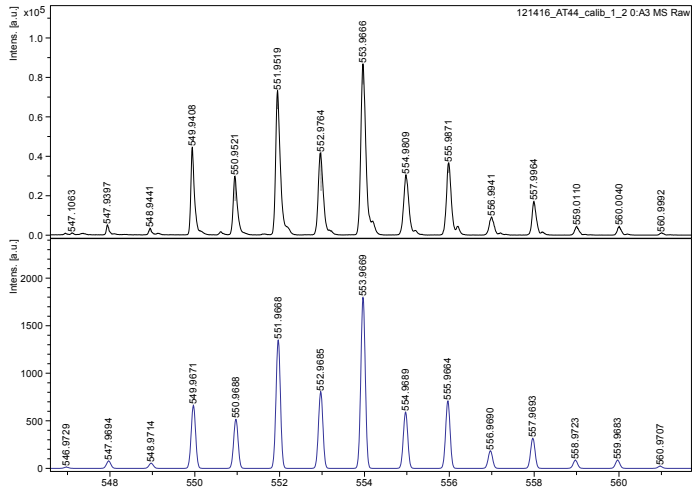

Figure S36. MALDI-TOF mass spectrum of (p*S*)-**4**.

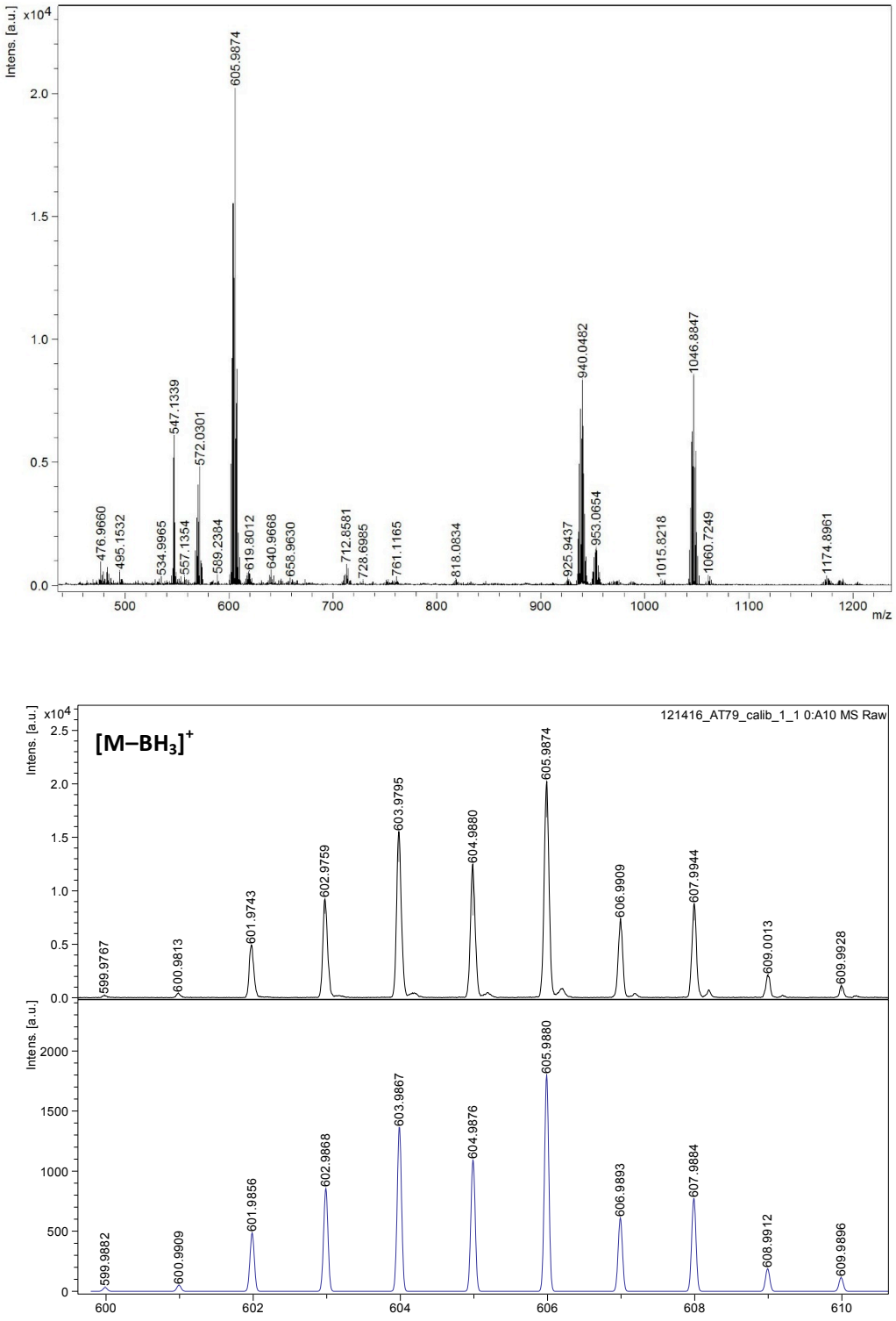

Figure S37. MALDI-TOF mass spectrum of *rac*-**5**; the additional peaks at higher molecular weight correspond to [*rac*-**6**–BH_3]$^+$ (940.0842 Da) and an undetermined dimeric species.

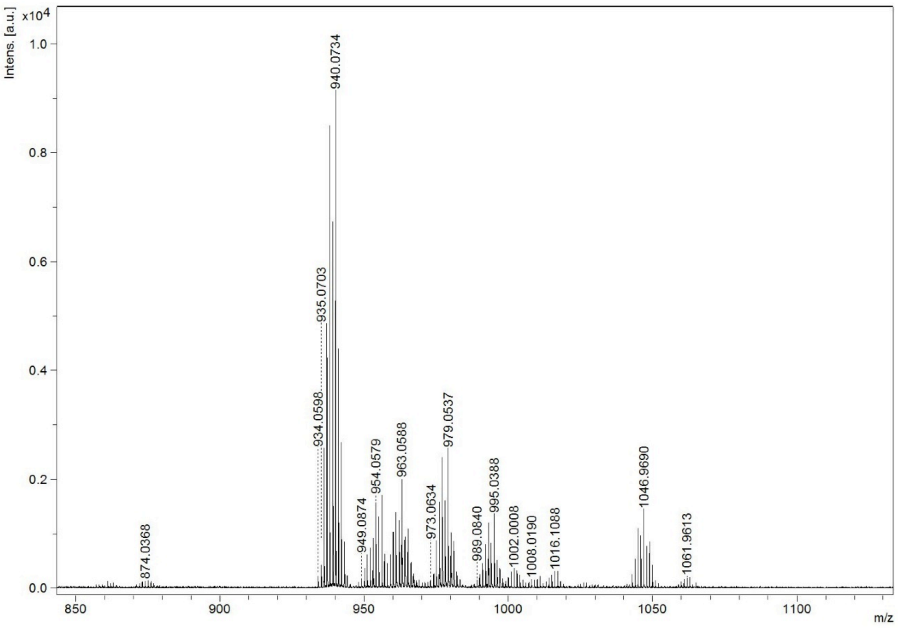

[M–BH$_3$]$^+$

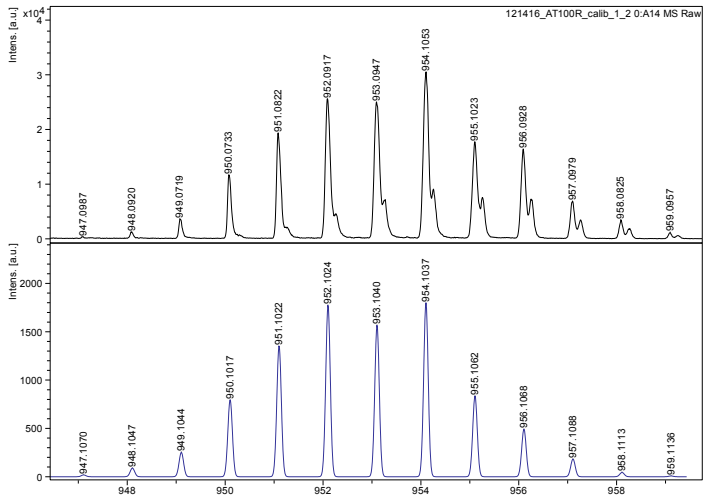

[M–2BH$_3$]$^+$

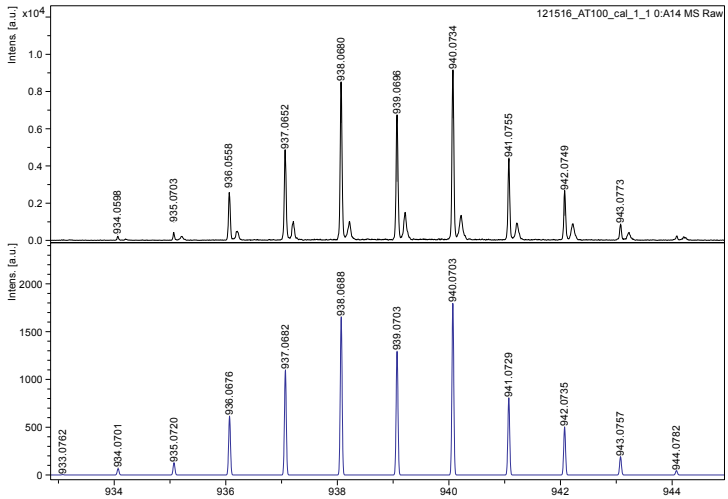

Figure S38. MALDI-TOF mass spectrum of (p*Sp*,*S*)-**6**.

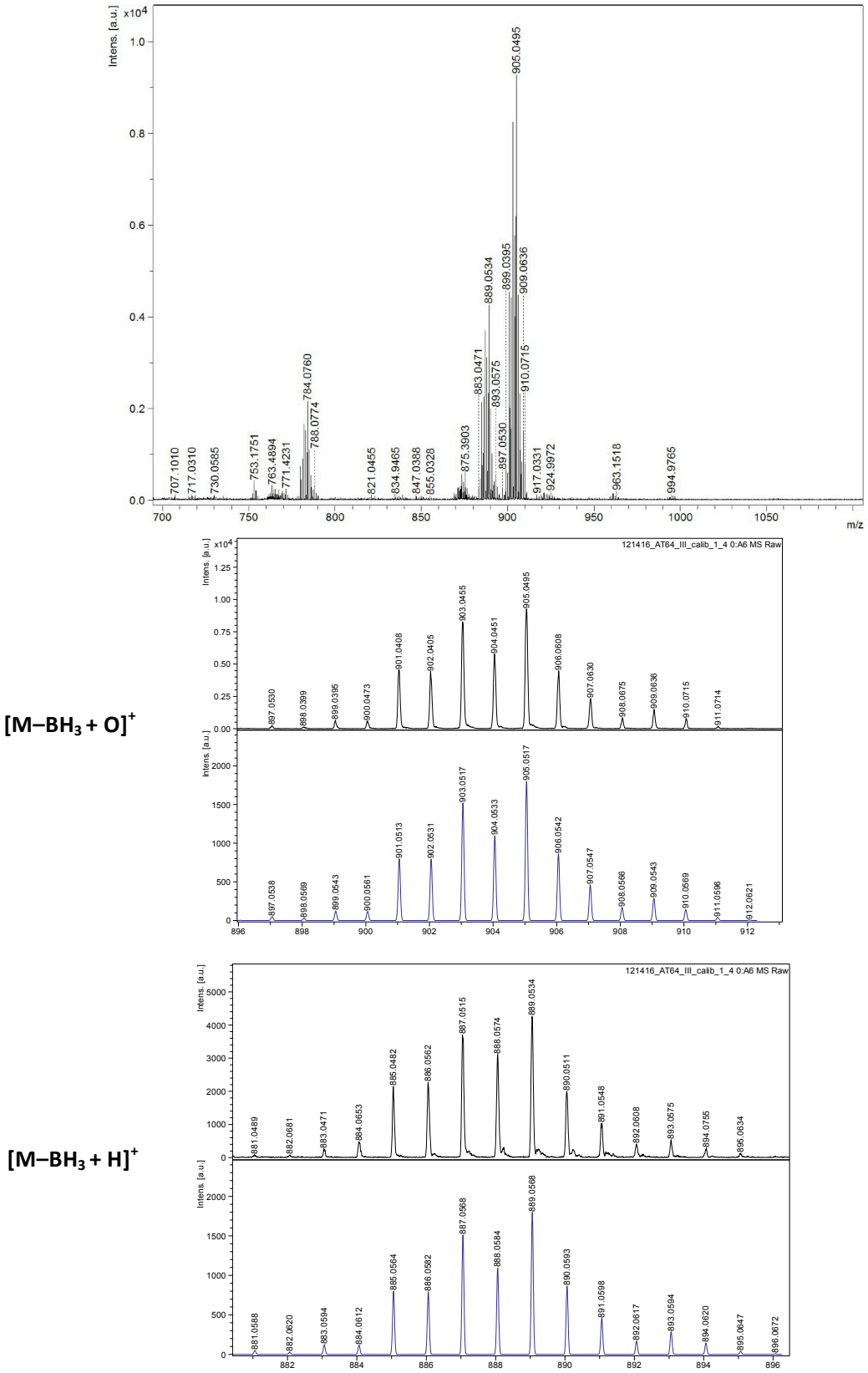

Figure S39. MALDI-TOF mass spectrum of (p*S*p*S*)-**7**.

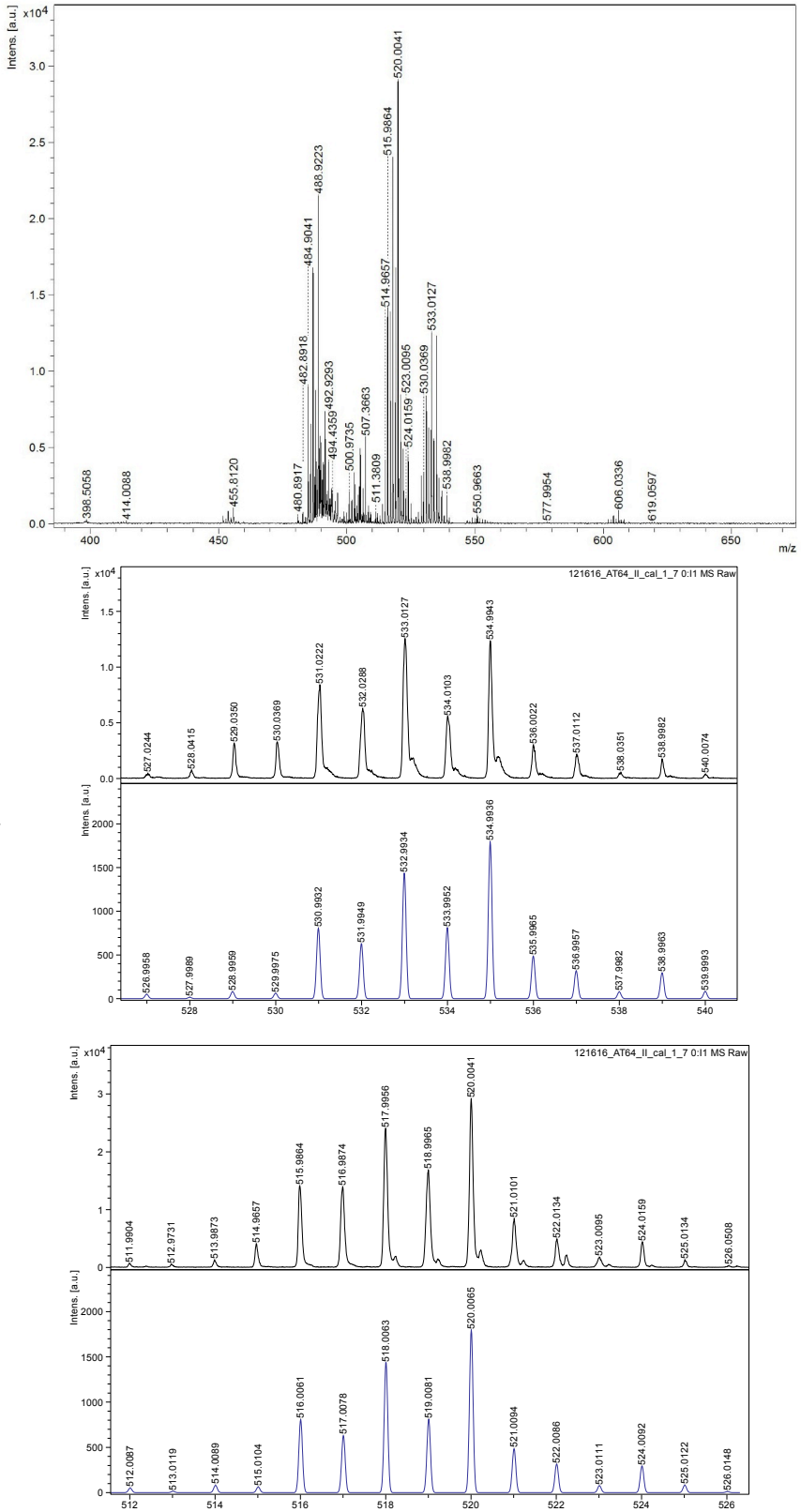

[M–BH$_3$–H + O]$^+$

[M–BH$_3$]$^+$

Figure S40. MALDI-TOF mass spectrum of (p*S*)-**8**.

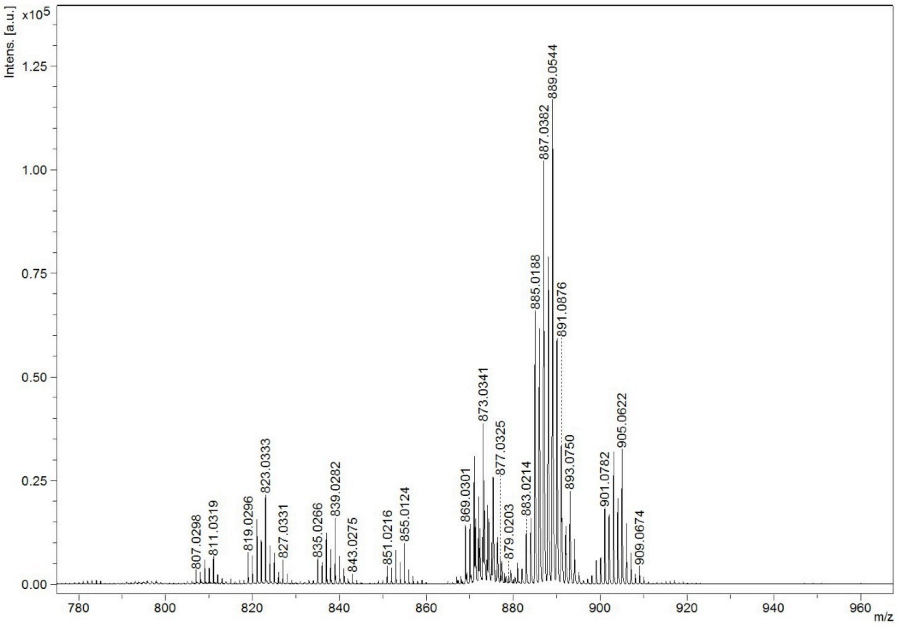

[M–2BH$_3$ + O]$^+$

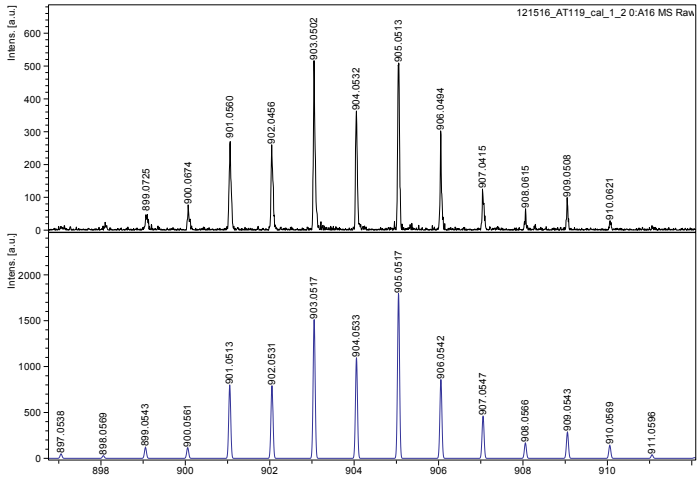

[M–2BH$_3$ + H]$^+$

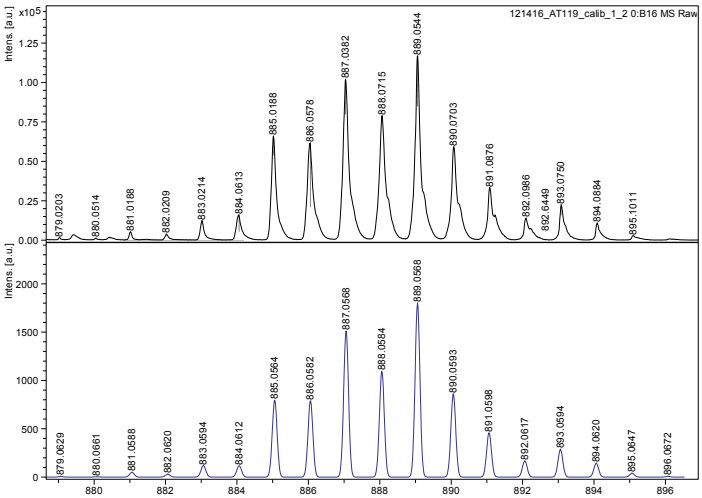

Figure S41. MALDI-TOF mass spectrum of (p*R*p*R*)-**10**.

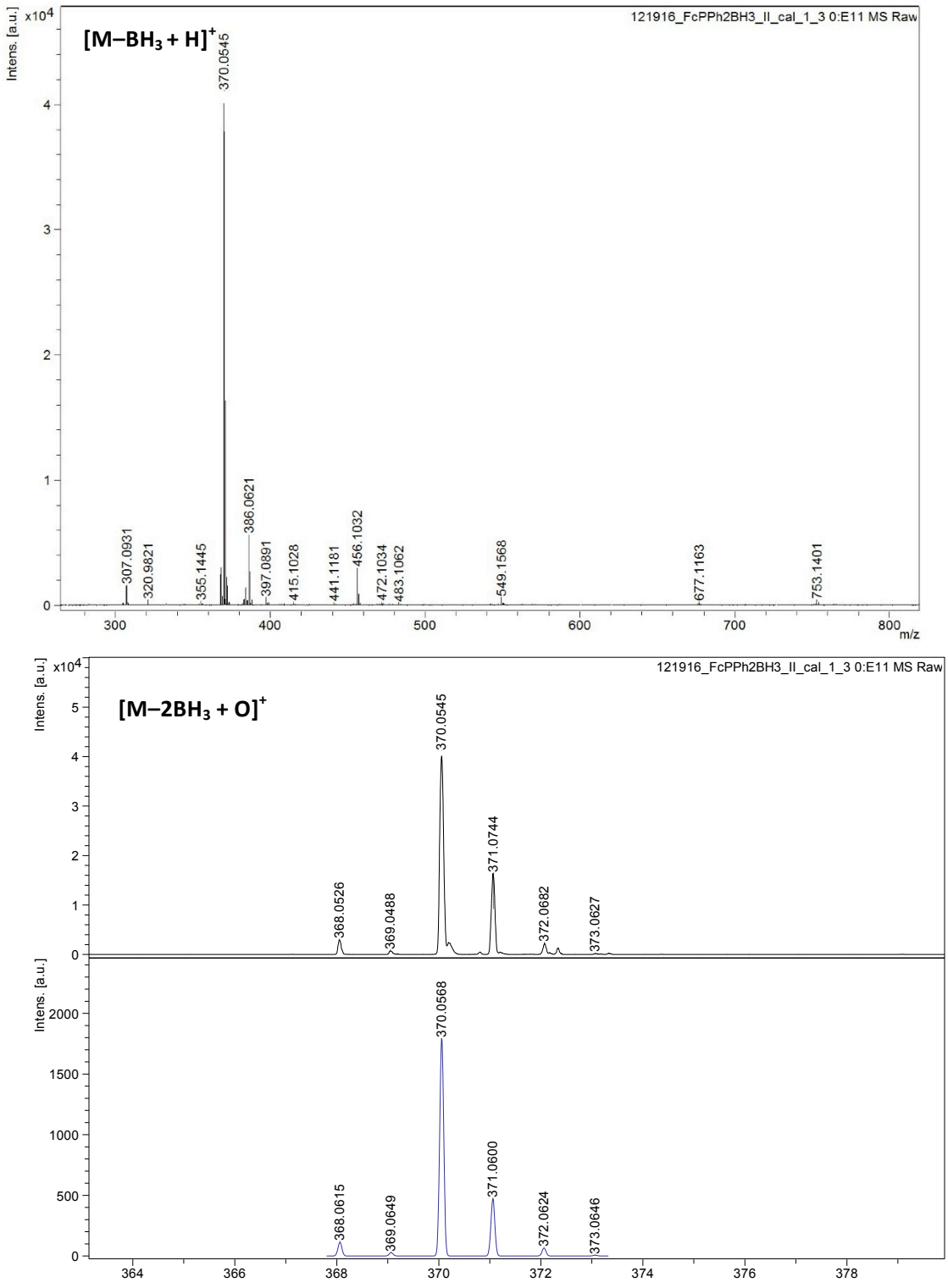

Figure S42. MALDI-TOF mass spectrum of **$FcPPh_2 \cdot BH_3$**.

Table S1. Crystal data and structure refinement details for (p*S*)-**3**, (p*S*)-**4**, *rac*-**5**, and (p*S*p*S*)-**7**.

Compound	(p*S*)-**3**	(p*S*)-**4**	*rac*-**5**	(p*S*p*S*)-**7**
empirical formula	$C_{25}H_{30}BFePSn$	$C_{24}H_{27}BClFePSn$	$C_{22}H_{21}BClFeHg\ P$	$C_{46}H_{45}BFe_2P_2Sn$
MW	546.81	567.22	619.06	900.96
T, K	100	100	100	100
wavelength, Å	1.54178	1.54178	1.54178	1.54178
crystal system	Orthorhombic	Orthorhombic	Orthorhombic	Orthorhombic
space group	$P2_12_12_1$	$P2_12_12_1$	*P*bca	$P2_12_12_1$
a, Å	7.4543(2)	7.3385(2)	15.7369(8)	10.8780(2)
b, Å	16.4141(4)	16.5867(4)	15.0095(7)	17.5543(4)
c, Å	19.3128(4)	19.1137(5)	17.5758(8)	20.7334(5)
α, deg	90	90	90	90
β, deg	90	90	90	90
γ, deg	90	90	90	90
V, Å^3	2363.0(1)	2326.5(1)	4151.5(3)	3959.16(15)
Z	4	4	8	4
ρ_{calc}, g cm^{-3}	1.537	1.619	1.981	1.512
μ (Cu Kα), mm^{-1}	14.01	15.29	20.61	11.78
crystal size, mm	0.38×0.21×0.18	0.26×0.21×0.07	0.26×0.18×0.11	0.29×0.23×0.17
θ range, deg	3.5–70.5	3.5–69.5	4.8–68.7	3.3–68.8
limiting indices	$-8 \le h \le 8$ $-20 \le k \le 19$ $-23 \le l \le 22$	$-6 \le h \le 8$ $-20 \le k \le 18$ $-21 \le l \le 23$	$-16 \le h \le 17$ $-17 \le k \le 18$ $-20 \le l \le 20$	$-12 \le h \le 12$ $-20 \le k \le 21$ $-24 \le l \le 24$
reflns collected	21972	15955	36723	34745
independent reflns	4183 [R(int) = 0.036]	3813 [R(int) = 0.026]	3696 [R(int) = 0.040]	6872 [R(int) = 0.050]
absorption correction	Numerical	Numerical	Numerical	Numerical
data/restraints/parameters	4183/3/274	3813/0/273	3696/0/256	6872/3/480
goodness-of-fit on F^2	1.05	1.03	1.13	0.98
final R indices, [I >2σ(I)] [a]	0.016, w$R2$ = 0.040	0.018, w$R2$ = 0.038	0.022, w$R2$ = 0.067	0.021, w$R2$ = 0.044
R indices (all data) [a]	0.017	0.019	0.0256	0.022
peak$_{max}$/hole$_{min}$ (e Å^{-3})	0.38 / –0.35	0.50 / –0.41	0.83 / –1.15	0.27 / –0.31
absolute structure parameter	0.038(3)	0.020(3)	-	0.027(2)

[a] $R1 = \Sigma||F_o|-|F_c||/\Sigma|F_o|$; $wR2 = \{\Sigma[w(F_o^2-F_c^2)^2]/\Sigma[w(F_o^2)^2]\}^{1/2}$

Computational Details for the Optimized Structures of (p*S*)-3 and (p*S*)-4

Compound (p*S*)-3

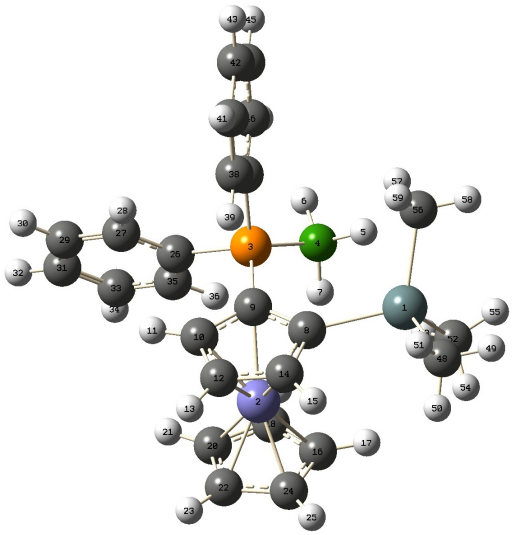

Stoichiometry $C_{25}H_{30}BFePSn$
Framework group C1[X($C_{25}H_{30}BFePSn$)]
Deg. of freedom 171
Full point group C1 NOp 1
Largest Abelian subgroup C1 NOp 1
Largest concise Abelian subgroup C1 NOp 1

Selected Distances:
H1···Sn1 = 3.129 Å, P1–B1 = 1.939 Å

Standard orientation:

Center Number	Atomic Number	Coordinates (Angstroms)		
		X	Y	Z
1	50	-2.58529	1.199284	0.337887
2	26	-0.790654	-1.935737	-0.611357
3	15	1.399948	0.439541	0.551407
4	5	0.739987	0.709201	2.337561
5	1	-0.091022	1.54001	2.151053
6	1	1.660059	1.215123	2.897112
7	1	0.398522	-0.358819	2.747869
8	6	-1.170403	0.07523	-0.810315
9	6	0.263758	-0.185455	-0.683922
10	6	0.655404	-1.062638	-1.769566
11	1	1.57566	-1.42283	-1.932356
12	6	-0.498517	-1.331822	-2.559508
13	1	-0.535087	-1.916885	-3.369736
14	6	-1.592088	-0.638033	-1.97695
15	1	-2.531896	-0.673382	-2.312814
16	6	-1.957743	-2.622607	0.930012
17	1	-2.604682	-2.076636	1.462663
18	6	-0.589706	-2.819927	1.234482
19	1	-0.103202	-2.435735	2.018957
20	6	-0.024525	-3.648508	0.22594
21	1	0.926355	-3.956572	0.177106
22	6	-1.050772	-3.954385	-0.702215
23	1	-0.952316	-4.521314	-1.520511
24	6	-2.250903	-3.322901	-0.267319
25	1	-3.140851	-3.367902	-0.721499
26	6	2.837419	-0.679918	0.453404
27	6	3.763507	-0.580296	-0.588939
28	1	3.664508	0.095568	-1.249582
29	6	4.826001	-1.463959	-0.657907
30	1	5.443169	-1.407464	-1.377637
31	6	4.993319	-2.437421	0.32516

32	1	5.731654	-3.034477	0.284395
33	6	4.086155	-2.527813	1.356291
34	1	4.202716	-3.189376	2.027935
35	6	2.997506	-1.661788	1.423586
36	1	2.36777	-1.740552	2.131064
37	6	2.024339	2.03581	-0.066649
38	6	1.291715	2.826815	-0.936768
39	1	0.47601	2.496789	-1.296752
40	6	1.732783	4.09086	-1.290692
41	1	1.216565	4.627576	-1.880302
42	6	2.930994	4.576753	-0.779261
43	1	3.238723	5.442151	-1.022571
44	6	3.674737	3.791711	0.08608
45	1	4.498531	4.119828	0.428179
46	6	3.231018	2.530027	0.458346
47	1	3.739736	2.004961	1.06451
48	6	-4.412613	0.876052	-0.758687
49	1	-5.167185	1.243732	-0.252387
50	1	-4.545997	-0.085714	-0.892856
51	1	-4.35292	1.322257	-1.629088
52	6	-2.91545	0.560593	2.368493
53	1	-2.167507	-0.002804	2.658403
54	1	-3.750285	0.046688	2.417337
55	1	-2.978767	1.344524	2.951408
56	6	-2.046557	3.267888	0.334065
57	1	-1.163399	3.375373	0.743673
58	1	-2.707308	3.778643	0.844827
59	1	-2.02146	3.597443	-0.589347

Compound (p*S*)-4

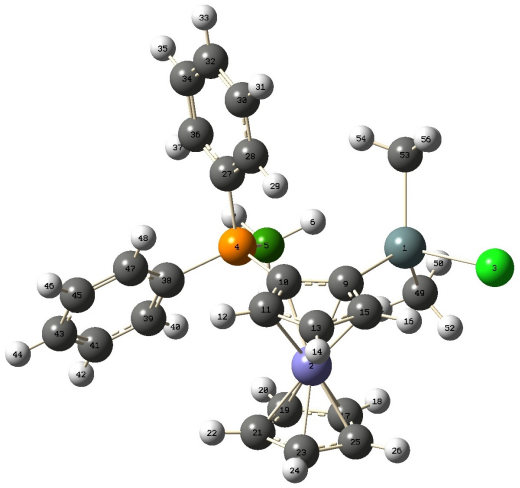

Stoichiometry $C_{24}H_{27}BClFePSn$
Framework group C1[X($C_{24}H_{27}BClFePSn$)]
Deg. of freedom 162
Full point group C1 NOp 1
Largest Abelian subgroup C1 NOp 1
Largest concise Abelian subgroup C1 NOp 1

Selected Distances:
H1···Sn1 = 2.631 Å, P1–B1 = 1.944 Å

Standard orientation:

Center Number	Atomic Number	Coordinates (Angstroms)		
		X	Y	Z
1	50	-2.387491	1.053314	0.483656
2	26	-0.581954	-1.988349	-0.608665
3	17	-4.413978	0.647573	-0.741682
4	15	1.506943	0.497409	0.486467
5	5	0.731641	0.783261	2.225411
6	1	-0.135303	1.493664	1.988938
7	1	1.559874	1.289407	2.768124
8	1	0.454398	-0.182868	2.686438
9	6	-1.051563	-0.007618	-0.796202
10	6	0.380792	-0.192745	-0.724452
11	6	0.768098	-1.053679	-1.82369
12	1	1.695888	-1.370848	-2.021881
13	6	-0.392187	-1.37801	-2.560602
14	1	-0.429195	-1.969557	-3.365233
15	6	-1.503912	-0.740575	-1.944024
16	1	-2.454978	-0.815386	-2.246204
17	6	-1.745885	-2.757035	0.892977
18	1	-2.458775	-2.260495	1.38665
19	6	-0.389626	-2.826751	1.265923
20	1	0.025492	-2.395025	2.064962
21	6	0.28166	-3.607091	0.297166
22	1	1.257278	-3.826917	0.296554
23	6	-0.666676	-4.02463	-0.677975
24	1	-0.479761	-4.597013	-1.476591
25	6	-1.93308	-3.48983	-0.299277
26	1	-2.797622	-3.615034	-0.78561
27	6	2.066287	2.1125	-0.133623
28	6	1.232687	2.92263	-0.892193

29	1	0.400481	2.584349	-1.2042
30	6	1.606482	4.225473	-1.202454
31	1	1.030393	4.77083	-1.725891
32	6	2.807298	4.730431	-0.750716
33	1	3.054246	5.625762	-0.951504
34	6	3.658284	3.921068	0.000565
35	1	4.496516	4.256278	0.293698
36	6	3.278619	2.629793	0.31862
37	1	3.850403	2.091511	0.852564
38	6	2.971578	-0.569082	0.426114
39	6	3.191457	-1.48142	1.436744
40	1	2.579852	-1.541903	2.161109
41	6	4.305864	-2.314384	1.399448
42	1	4.456598	-2.932401	2.1063
43	6	5.191114	-2.253965	0.346876
44	1	5.94783	-2.826981	0.322829
45	6	4.968048	-1.346089	-0.678138
46	1	5.564936	-1.310459	-1.41635
47	6	3.880512	-0.494362	-0.632667
48	1	3.748843	0.143066	-1.323557
49	6	-2.868549	0.319819	2.440408
50	1	-2.84552	1.060101	3.081112
51	1	-2.213835	-0.36047	2.703667
52	1	-3.76467	-0.077096	2.428536
53	6	-2.175888	3.165855	0.33518
54	1	-1.269819	3.423756	0.605279
55	1	-2.828189	3.601773	0.924183
56	1	-2.333224	3.445351	-0.590963

Second Order Perturbation Theory Analysis of Fock Matrix in NBO Basis

Compound (p*S*)-3:

Donor NBO (i)		Acceptor NBO (j)	E(2) kcal/mol	E(j)-E(i) a.u.	F(i,j) a.u.
8. BD (1) B4 - H5	/	133. LP*(1)Sn1	0.20	0.40	0.009

Compound (p*S*)-4:

Donor NBO (i)		Acceptor NBO (j)	E(2) kcal/mol	E(j)-E(i) a.u.	F(i,j) a.u.
7. BD (1) B5 - H6	/	134. LP*(2)Sn1	5.46	0.37	0.043

Atoms in Molecules (AIM) Analysis of Compound (p*S*)-4:

Electron Density and Laplacian of the Electron Density at the BCPs:

BCP	#	Name	Atoms	Rho	DelSqRho	Ellipticity	K	BPL - GBL_I
1	1	BCP1	Sn1-C9	0.058257	+0.441543	0.098363	+0.003085	0.000321
2	2	BCP2	Sn1-Cl3	0.031057	+0.263762	0.180649	+0.000203	0.001279
3	3	BCP3	Sn1-H6	0.008196	+0.040694	3.173225	-0.001239	0.027879
4	4	BCP4	P4-B5	0.117967	-0.123341	0.015182	+0.091664	0.000114
5	5	BCP5	B5-H6	0.163606	-0.186163	0.031616	+0.152568	0.000261
6	6	BCP6	B5-H7	0.167393	-0.261977	0.015456	+0.157056	0.000111
7	7	BCP7	B5-H8	0.165492	-0.233826	0.024250	+0.155217	0.000133
8	8	BCP8	Cl3-H16	0.006648	+0.026096	0.304853	-0.001318	0.109756
9	9	BCP9	Fe2-C10	0.053785	+0.263912	1.829033	+0.015711	0.379691
10	10	BCP10	P4-C10	0.167724	-0.281002	0.033883	+0.165734	0.001202
11	11	BCP11	C9-C10	0.282342	-0.794933	0.036028	+0.273013	0.020816
12	12	BCP12	C10-C11	0.291520	-0.729070	0.485689	+0.290491	0.009605
13	13	BCP13	C11-H12	0.279412	-0.986564	0.019557	+0.279439	0.001116
14	14	BCP14	C11-C13	0.295221	-0.823018	0.149306	+0.305908	0.089367
15	15	BCP15	Fe2-C13	0.049639	+0.369907	0.128523	+0.010907	0.170992
16	16	BCP16	C13-C15	0.294591	-0.824166	0.162673	+0.304573	0.087089
17	17	BCP17	C13-H14	0.277657	-0.885774	0.142848	+0.275465	0.010568
18	18	BCP18	Fe2-C9	0.053177	+0.250908	1.486597	+0.017293	0.272246
19	19	BCP19	C9-C15	0.296944	-0.735719	0.420427	+0.301185	0.023736
20	20	BCP20	C15-H16	0.280408	-0.981077	0.025007	+0.278860	0.000970
21	21	BCP21	Fe2-C19	0.049804	+0.265852	1.730782	+0.013919	0.951930
22	22	BCP22	Fe2-C21	0.049772	+0.274336	1.635907	+0.013260	1.013026
23	23	BCP23	C17-H18	0.279963	-0.983094	0.024664	+0.280751	0.001585
24	24	BCP24	H20-H40	0.003597	+0.012389	0.850014	-0.000924	0.383545
25	25	BCP25	H8-H20	0.005453	+0.018013	0.104974	-0.001096	0.077273
26	26	BCP26	Fe2-C25	0.051402	+0.381232	0.074650	+0.011728	0.146277
27	27	BCP27	C17-C19	0.301656	-0.801494	0.508203	+0.308525	0.011939
28	28	BCP28	C19-H20	0.280003	-0.985321	0.024571	+0.280537	0.001692
29	29	BCP29	C21-C23	0.300241	-0.794696	0.507503	+0.305909	0.012389
30	30	BCP30	C19-C21	0.293798	-0.952076	0.057943	+0.298352	0.002183
31	31	BCP31	C21-H22	0.278303	-0.975457	0.025058	+0.277941	0.001693
32	32	BCP32	C23-C25	0.293044	-0.799945	0.165894	+0.300031	0.089186
33	33	BCP33	C17-C25	0.293775	-0.806941	0.164471	+0.301336	0.088000
34	34	BCP34	C23-H24	0.277909	-0.972062	0.023815	+0.277608	0.001547
35	35	BCP35	C25-H26	0.277897	-0.888962	0.141866	+0.275800	0.009718
36	36	BCP36	P4-C27	0.163534	-0.301138	0.040719	+0.159916	0.000486
37	37	BCP37	C27-H54	0.002591	+0.006043	0.356704	-0.000427	0.248583
38	38	BCP38	C27-C28	0.299227	-0.812036	0.488411	+0.315439	0.000105
39	39	BCP39	C28-H29	0.280761	-0.988600	0.022208	+0.281177	0.000073
40	40	BCP40	C28-C30	0.304601	-1.061286	0.036974	+0.324759	0.000139
41	41	BCP41	C30-C32	0.304935	-0.871338	0.514585	+0.326585	0.000119

Experimental IR Spectral Data and Calculated Frequencies

ATR-FTIR analysis of compound (p*S*)-**3** revealed two strong and broad absorption bands at 2403 and 2378 cm^{-1} corresponding to the B–H stretching frequencies. These bands are significantly shifted to 2417 and 2314 cm^{-1} in the IR spectrum of (p*S*)-**4**. DFT frequency calculations of the optimized structures predict absorption bands for **3** at 2462, 2524, and 2538 cm^{-1}; and for (p*S*)-**4** at 2443, 2505 and 2546 cm^{-1}. According to the computed results, the B–H stretching frequencies involved in an agostic-type interaction with the tin atom are assigned to be those at 2538 ((p*S*)-**3**) and 2443 ((p*S*)-**4**) cm^{-1}, which suggests a bathochromic shift of 95 cm^{-1} that is similar to the bathochromic shift (89 cm^{-1}) when comparing the experimentally observed bands at 2403 cm^{-1} in (p*S*)-**3** and 2314 cm^{-1} in (p*S*)-**4**. The ATR-FTIR spectra of the parent compound **$FcPPh_2 \cdot BH_3$** showed a broad absorption band at 2380 cm^{-1}.

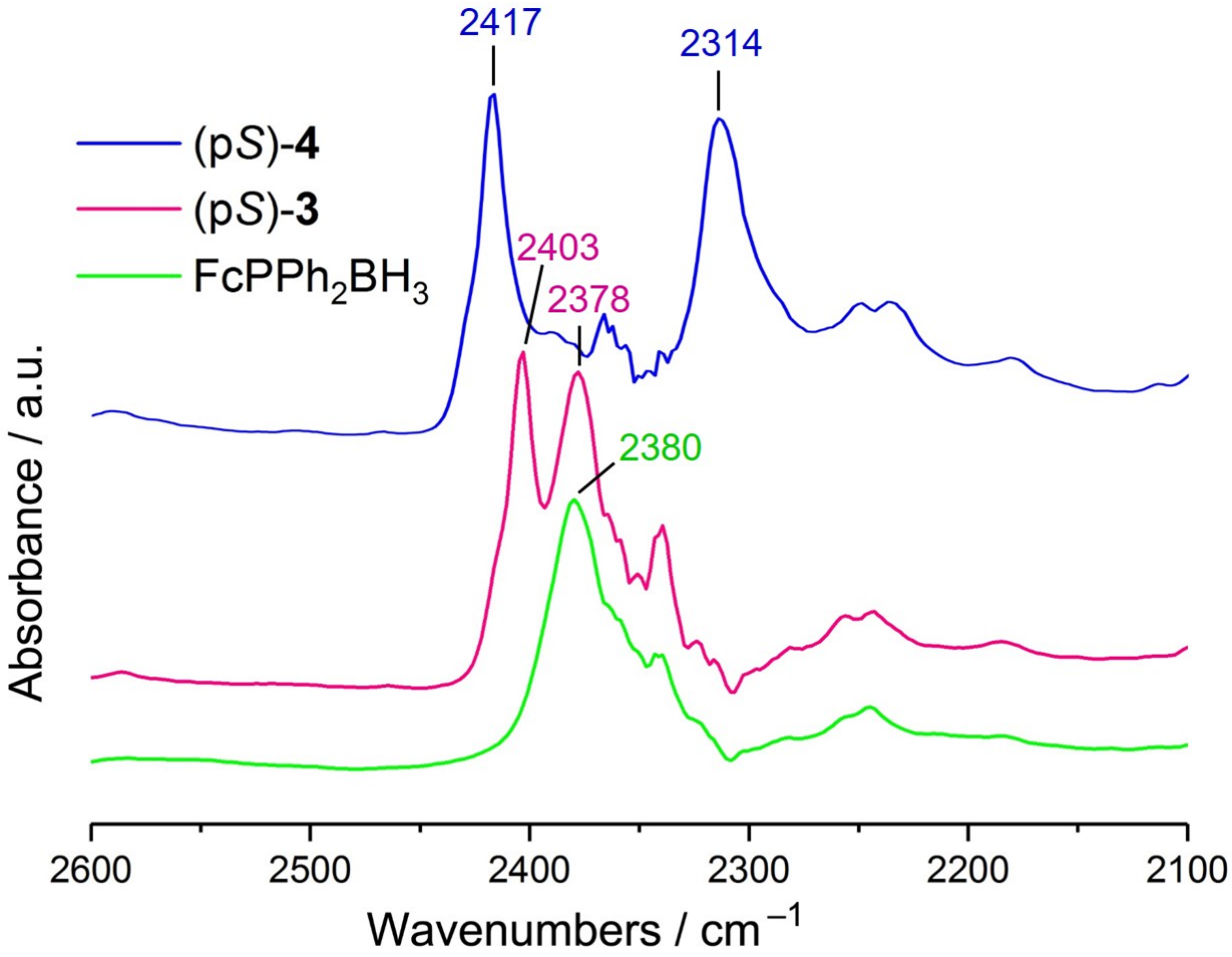

Calculated Frequencies for Compound (p*S*)-3:

Frequencies --	2461.5186	2523.5996	2538.2687
Red. masses --	1.0279	1.1106	1.1117
Frc consts --	3.6695	4.1673	4.2202
IR Inten --	44.7466	160.6705	139.2541

Atom	AN	X	Y	Z	X	Y	Z	X	Y	Z
4	5	0	-0.01	-0.04	-0.09	-0.05	-0.02	-0.05	0.09	-0.02
5	1	-0.36	0.31	-0.03	0.25	-0.23	0.01	0.62	-0.52	0.03
6	1	0.54	0.25	0.35	0.54	0.25	0.38	0.08	0.05	0.05
7	1	-0.15	-0.5	0.15	0.16	0.56	-0.19	-0.17	-0.52	0.17

Calculated Frequencies for Compound (p*S*)-4:

Frequencies --	2442.6894	2505.4818	2545.7510
Red. masses --	1.0442	1.0872	1.1146
Frc consts --	3.6709	4.0209	4.2561
IR Inten --	197.7806	163.3441	118.9582

Atom	AN	X	Y	Z	X	Y	Z	X	Y	Z
5	5	-0.05	0.03	0.01	0.06	-0.04	0.06	-0.05	-0.09	-0.01
6	1	0.73	-0.5	0.14	-0.34	0.23	-0.05	-0.03	0	0
7	1	-0.22	-0.15	-0.17	-0.44	-0.35	-0.38	0.44	0.32	0.38
8	1	0.06	0.29	-0.1	0.15	0.55	-0.2	0.16	0.68	-0.26

References:

1. M. A. Bennet, M. Contel, D. C. R. Hockless, L. L. Welling, A. C. Willis, *Inorg. Chem*. **2002**, *41*, 844-855.
2. The following van der Waals radii are used: H 1.10, B 1.92, O 1.52, P 1.80, Cl 1.75, Sn 2.17, Hg 2.05 Å; see M. Mantina, A. C. Chamberlin, R. Valero, C. J. Cramer, D. G. Truhlar *J. Phys. Chem. A*, **2009**, 113, 5806-5812; the value of 2.05 Å for Hg is taken from S. S. Batsanov, *J. Mol. Struct*. 1999, *468*, 151-159.